H_3^+ in Interstellar space

EPRP LS 2025 5AAA 11 03 2025

motto

If you understand hydrogen, you understand all that can be understood. V. Weisskopf (Taken from G. Herzberg).

Temperatures and energies

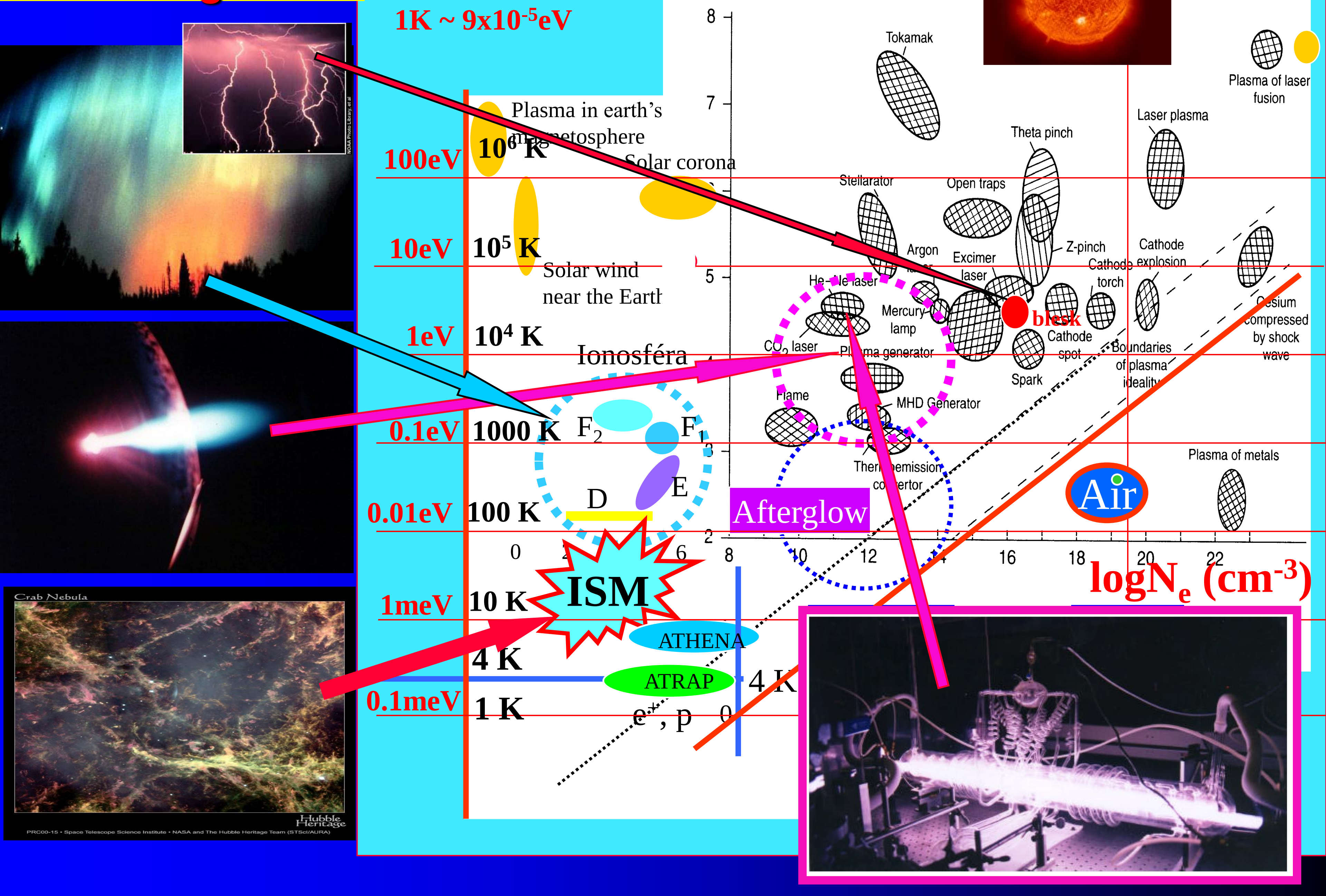

Electronvolt

***E*←→kT**
1eV ~ 11 604.505 K
1K ~ 9x10^{-5}eV

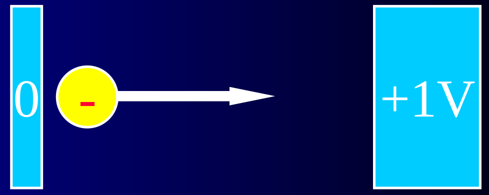

By definition, it is equal to the amount of kinetic energy gained by
a single unbound electron when it accelerates through an electric potential difference of one volt

Conversion factors:
1 eV = 1.6021765(40)×10^{-19}J (the conversion factor is numerically equal to the elementary charge expressed in coulombs).
1 eV (per atom) is 96.485 kJ/mol.

1.6 to 3.4 eV: the photon energy of visible light.

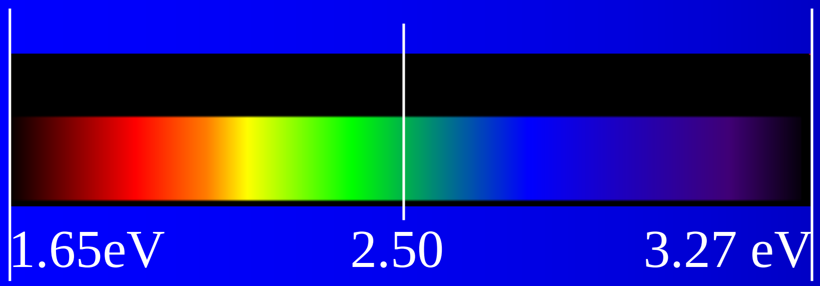

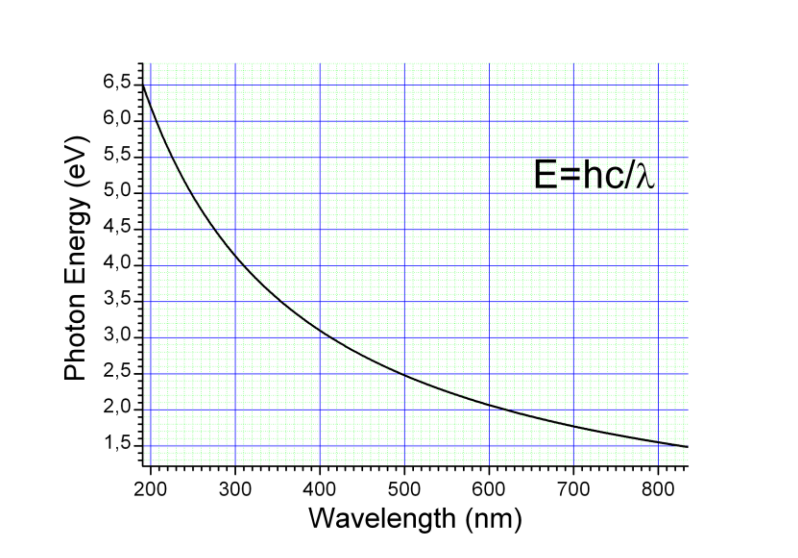

13.6 eV: The energy required to ionize atomic hydrogen.
Molecular bond energies are on the order of one eV per molecule

1 TeV: A trillion electronvolts, or 1.602×10^{-7} J, about the kinetic energy of a flying mosquito

14 TeV: the design proton collision energy at the Large Hadron Collider (which has operated at half of the energy since March 30, 2010).

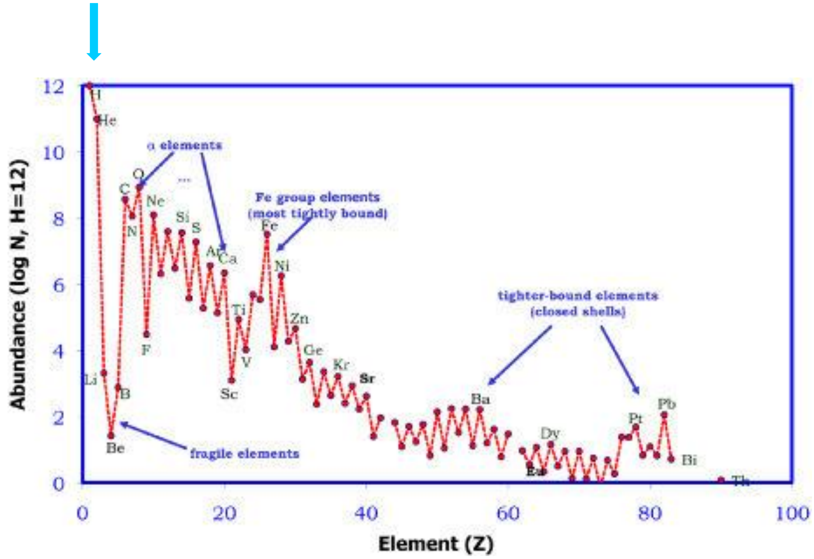

92.1% of nucleons in the universe are protons

7.8% are helium nuclei !

0.1%……C,N,O,S,Si….

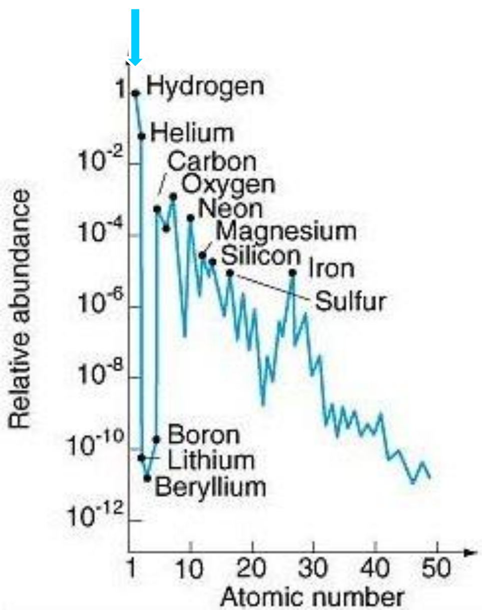

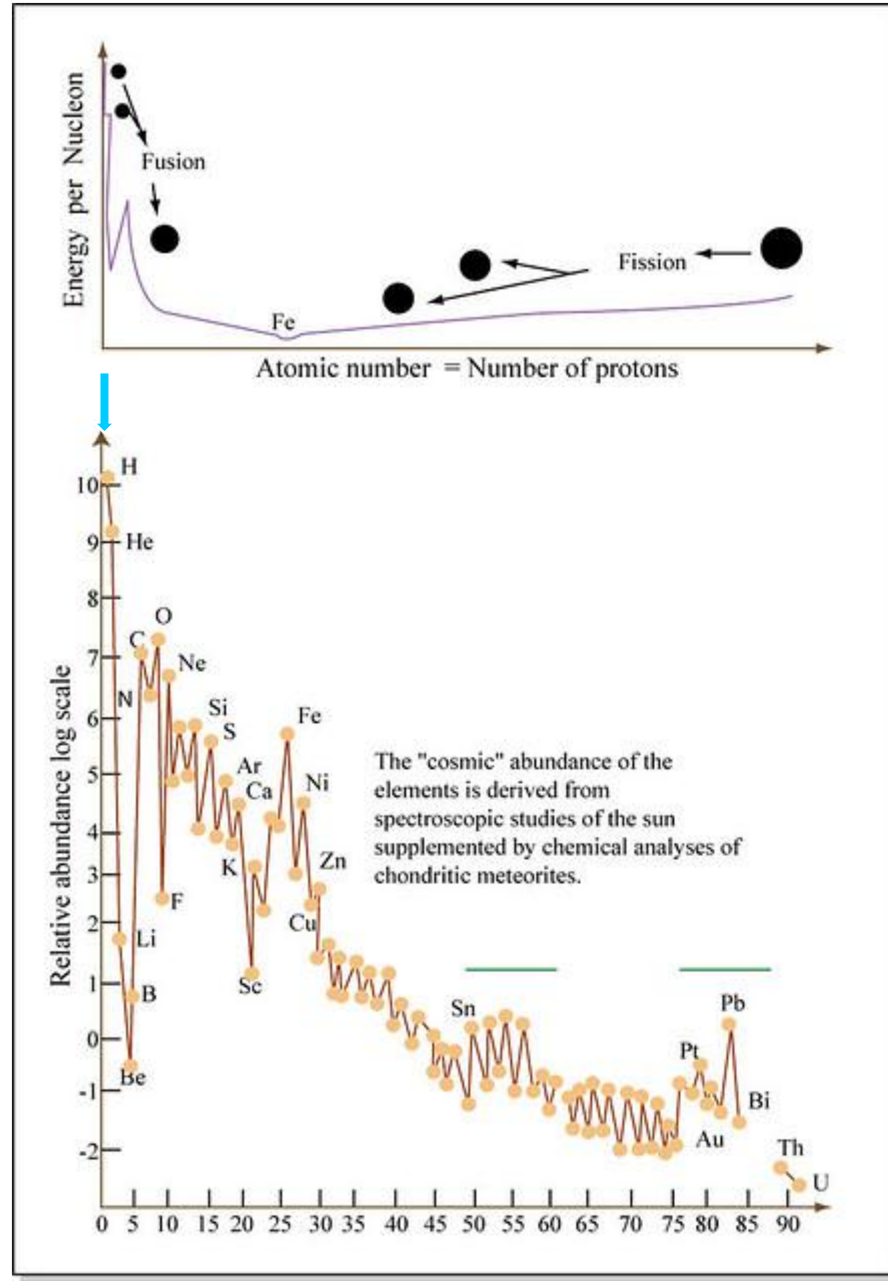

The cosmic elemental abundances extend over 12 orders of magnitude.

Interstellar medium

92.1% of nucleons in the universe are protons
7.8% are helium nuclei !
0.1%……C,N,O,S,Si….

Cosmic abundance

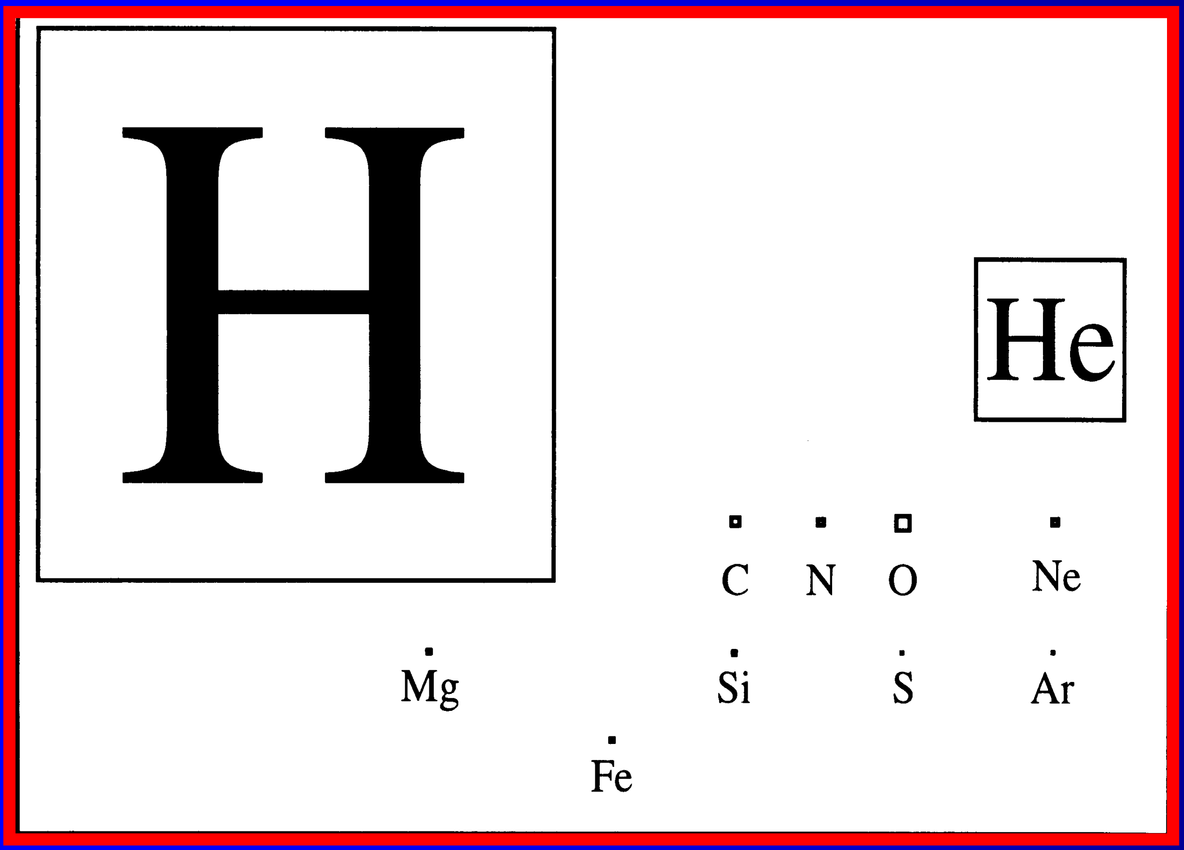

~0.005%……D

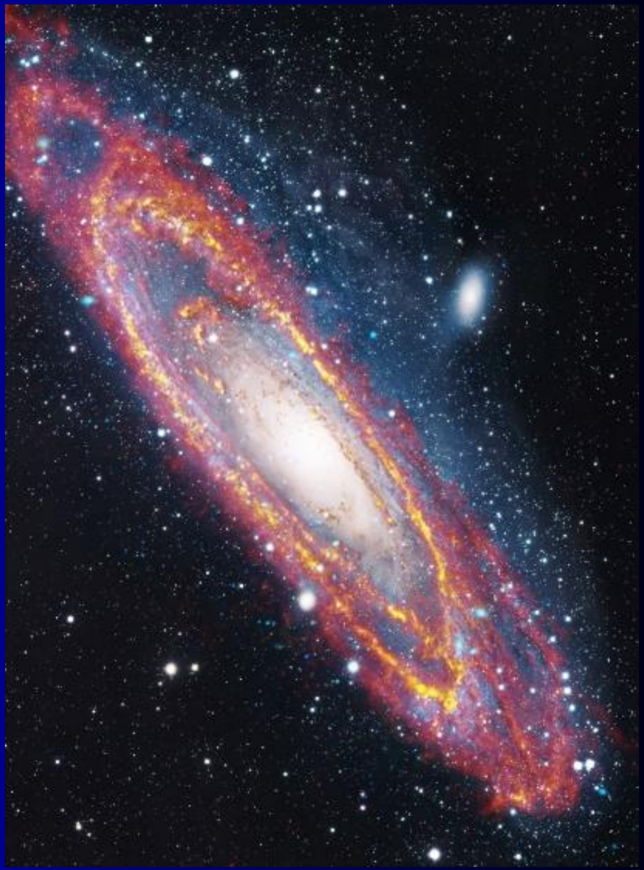

Andromeda composite

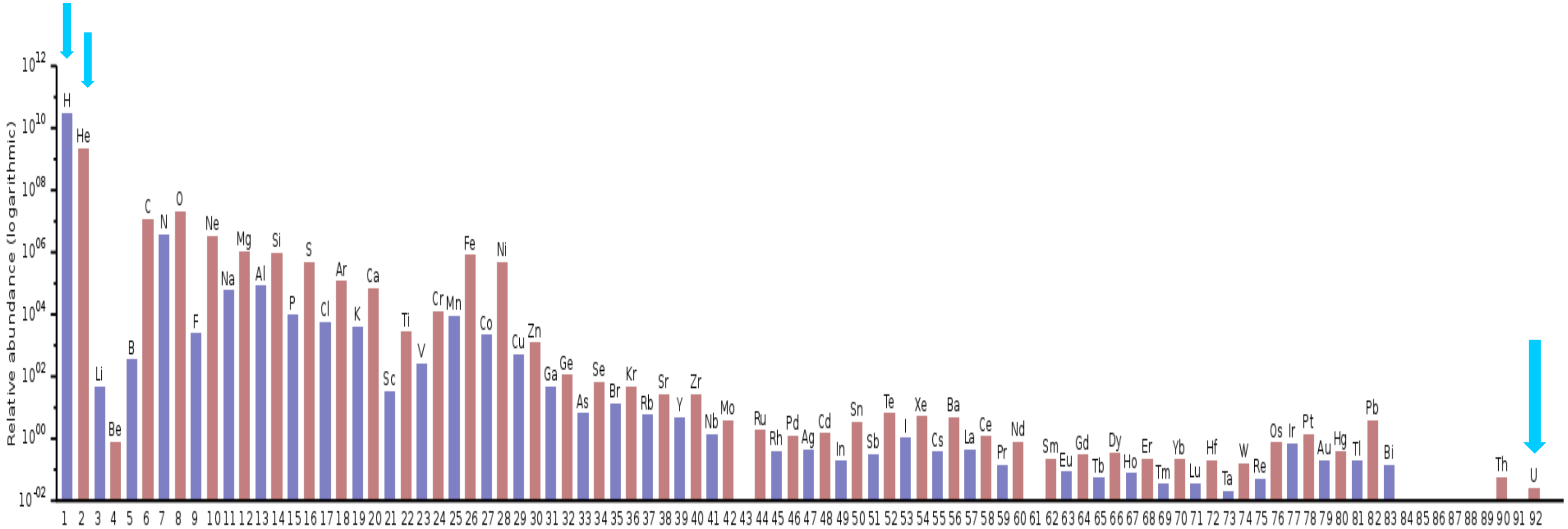

Estimated abundances of the chemical elements in the Solar System (logarithmic scale)

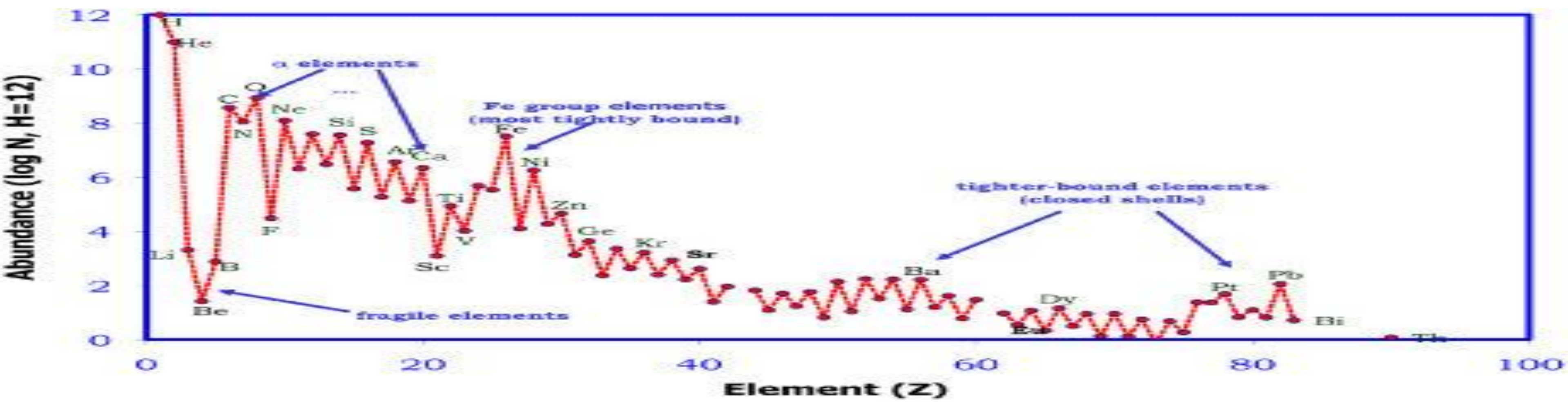

The cosmic elemental abundances extend over 12 orders of magnitude.

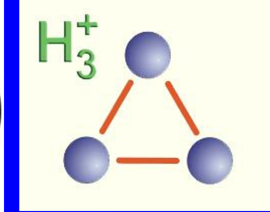

H_2 and H_3^+ Story

(IMR & Recombination of H_3^+)

motto

If you understand hydrogen, you understand all that can be understood. V. Weisskopf (Taken from G. Herzberg).

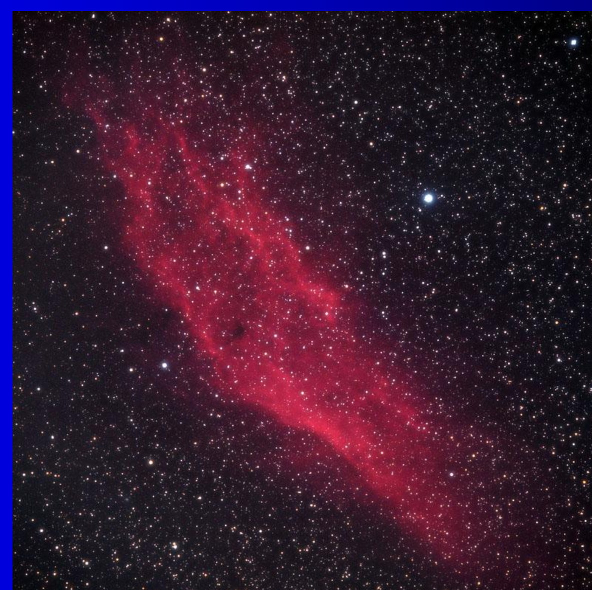

motivation?... $$$? ….

called Smith’s Cloud, after the astronomer who discovered it in 1963

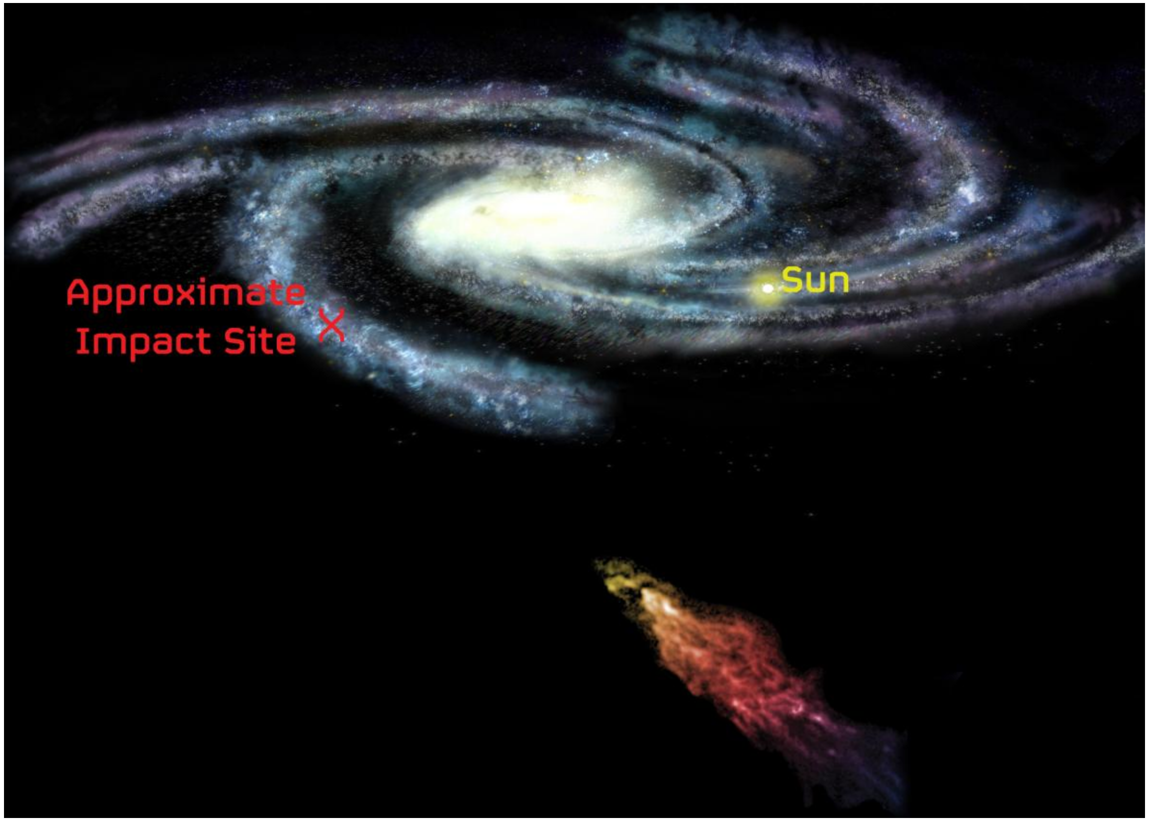

called Smith’s Cloud, after the astronomer who discovered it in 1963, contains enough hydrogen to make a million stars like the Sun. Eleven thousand light-years long and 2,500 light-years wide, it is only 8,000 light-years from our Galaxy’s disk. It is careening toward our Galaxy at more than 150 miles per second, aimed to strike the Milky Way’s disk at an angle of about 45 degrees. Don’t worry! It will hit 30,000 light years away from Earth.

.... What about energy…

Smith's Cloud

Our Galaxy will get a rain of gas from this cloud, then in about 20 to 40 million years, the cloud's core will smash into the Milky Way's plane," The cloud will likely strike a region somewhat farther from the Galactic center than our Solar System and about 90 degrees ahead of us in the Milky Way disk. The collision may trigger a period of rapid star formation fueled by the new gas and the shock from the collision. Some theories say that the ring of bright stars near the Sun, called Gould's Belt, was created by just such a collision event.

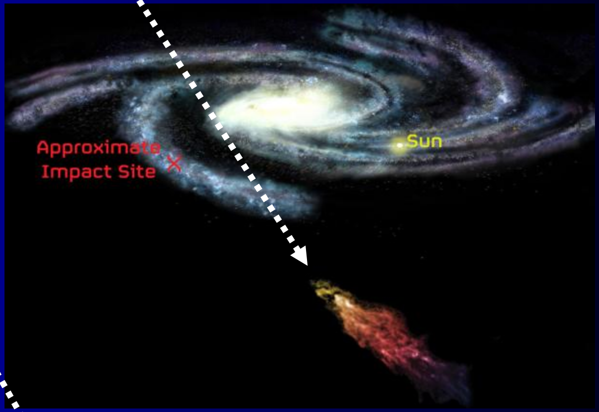

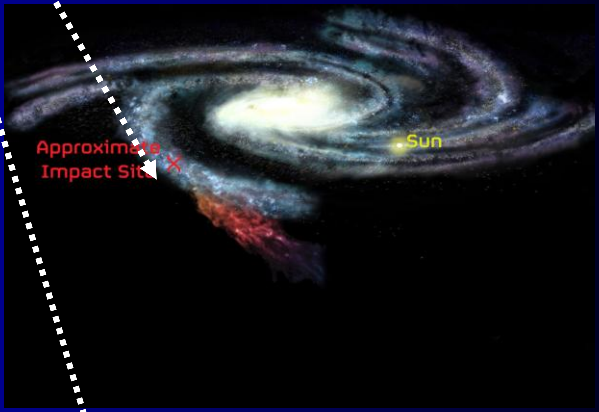

contains enough hydrogen to make a million stars like the Sun

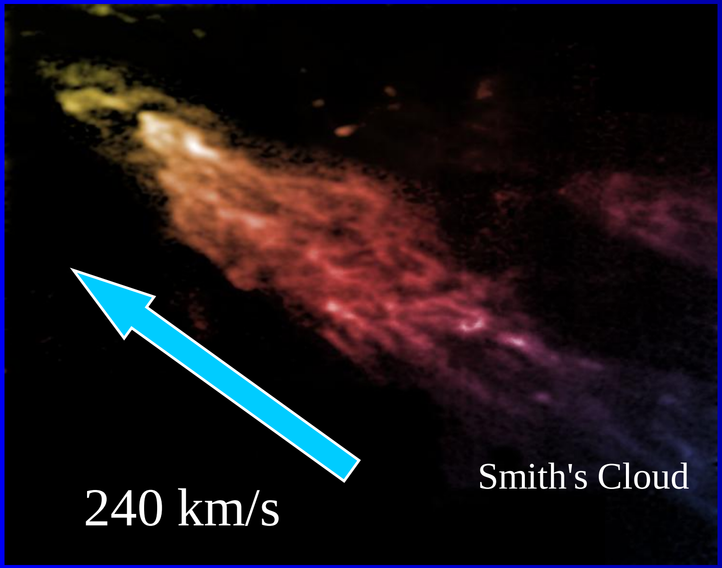

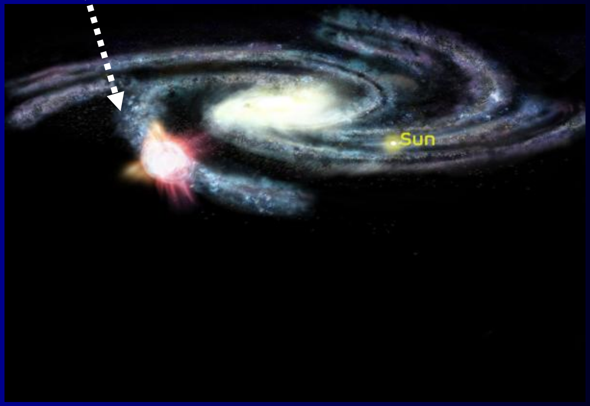

240 km/s ~562 eV ~$5x10^6$ K

Importance of Interstellar Hydrogen

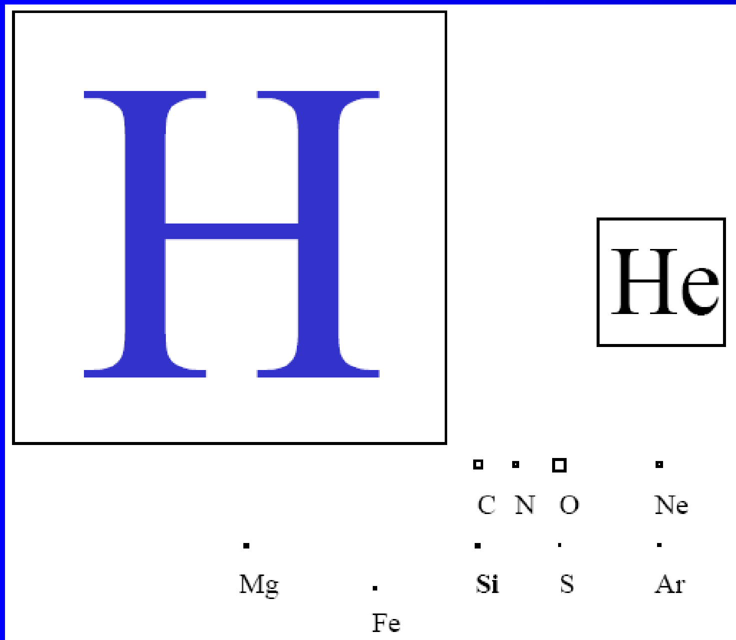

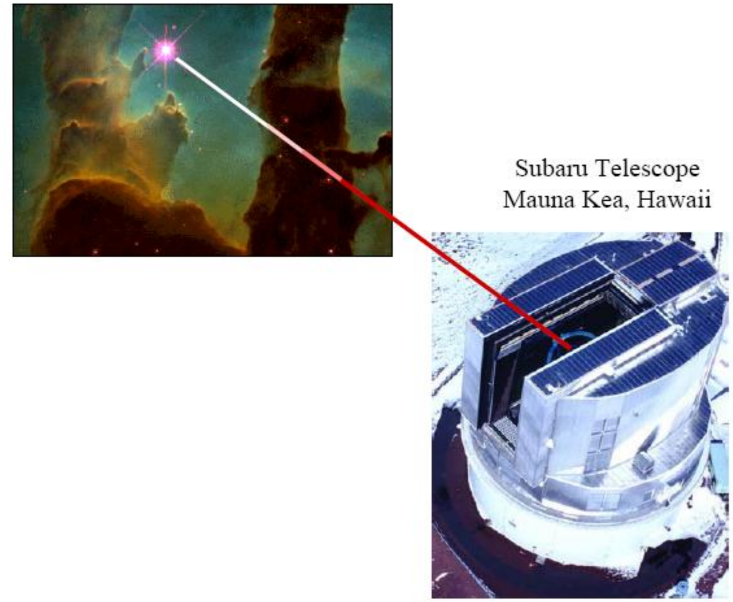

Subaru Telescope
Mauna Kea, Hawaii

Integrated area of absorption lines

United Kingdom Infrared Telescope
Mauna Kea, Hawaii

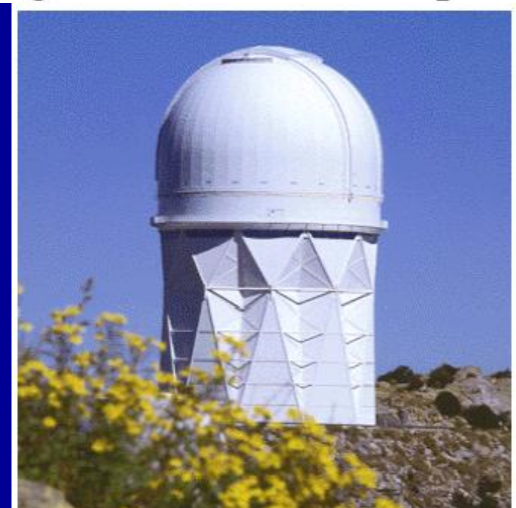

Nicholas U. Mayall Telescope
Kitt Peak, AZ

Importance of Interstellar H_3^+

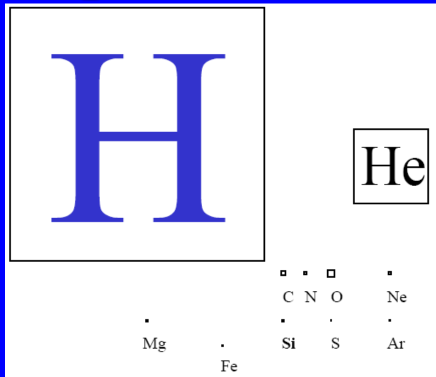

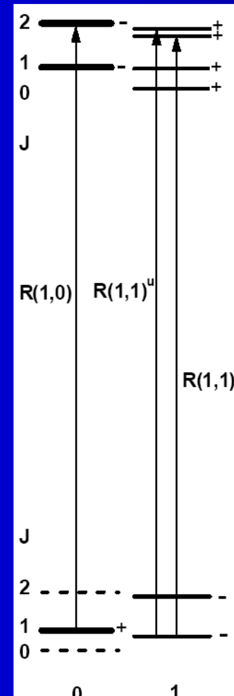

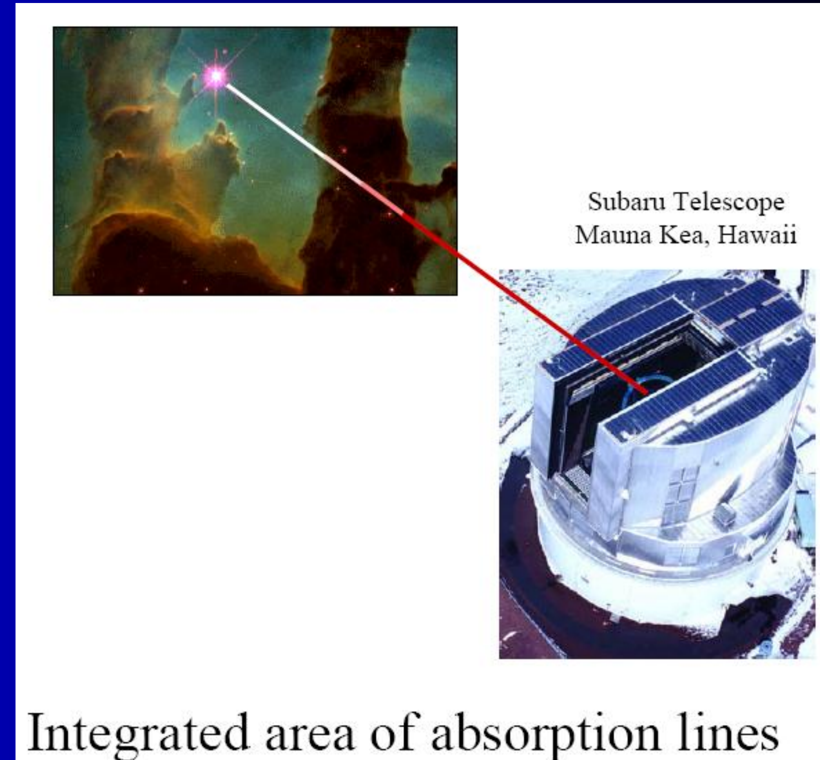

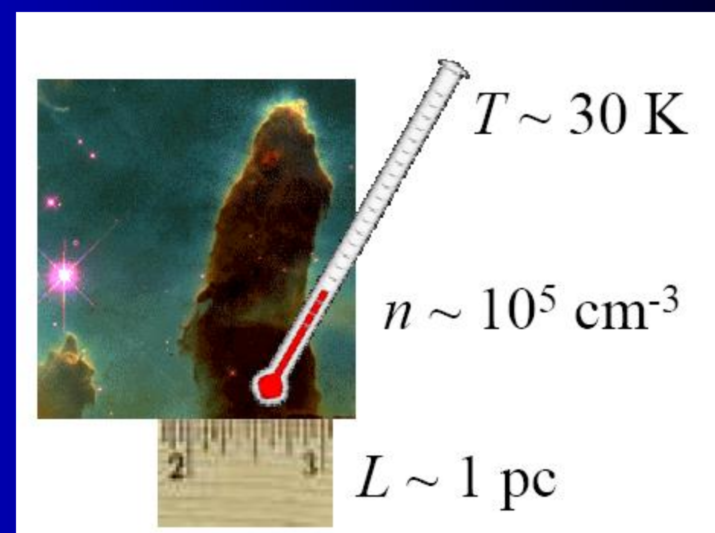

Table 2 Molecules detected in diffuse molecular clouds

Weight	Species	Method	Target	$N(X)/N_H$	Reference
2	H_2	UV	ζ Oph	0.56	1
3	HD	UV	ζ Oph	4.5 (−7)	2
3	H_3^+	IR	ζ Per	5.1 (−8)	3
13	CH	Optical	ζ Oph	1.5 (−9)	4
13	CH^+	Optical	ζ Oph	2.4 (−8)	5
14	$^{13}CH^+$	Optical	ζ Oph	3.5 (−10)	6
15	NH	Optical	ζ Oph	6.2 (−10)	7
17	OH	UV	ζ Oph	3.3 (−8)	8
24	C_2	Optical	ζ Oph	1.3 (−8)	9
25	C_2H	mm abs.	BL Lac	1.8 (−8)	10
26	CN	Optical	ζ Oph	1.9 (−9)	11
27	HCN	mm abs.	BL Lac	2.6 (−9)	12
27	HNC	mm abs.	BL Lac	4.4 (−10)	12
28	N_2	UV	HD 124314	3.1 (−8)	13
28	CO	UV	X Per	6.4 (−6)	14
29	HCO^+	mm abs.	BL Lac	1.5 (−9)	15
29	HOC^+	mm abs.	BL Lac	2.2 (−11)	15
29	^{13}CO	UV	X Per	8.9 (−8)	16
29	$C^{17}O$	UV	X Per	7.4 (−10):	16
30	$C^{18}O$	UV	X Per	2.1 (−9):	16
30	H_2CO	mm abs.	BL Lac	3.7 (−9)	17
36	C_3	Optical	ζ Oph	1.1 (−9)	18
36	HCl	UV	ζ Oph	1.9 (−10)	19
38	C_3H_2	mm abs.	BL Lac	6.4 (−10)	10
44	CS	mm abs.	BL Lac	1.6 (−9)	20
64	SO_2	mm abs.	BL Lac	≤8.2 (−10)	20

Plasma

Plasma.

+

e^-

Hydrogen containing molecules

H_2	H_3^+

Hydrogen + carbon containing molecules

CH	CH^+	CH_2	C_2	C_2H	C_3	C_2H_2	l - C_3H	c-C_3H
*CH_4	H_2CCC	c-C_3H_2	C_4H	*C_5	*C_2H_4	*C_5H	C_4H_2	l - H_2C_4
*C_6H	CH_3C_2H	*C_7H	C_6H_2	l - H_2C_6	*C_8H	CH_3C_4H	c-C_6H_6	

Hydrogen + oxygen + carbon containing molecules

OH	CO	CO^+	H_2O	HCO	HCO^+	HOC^+	C_2O	CO_2
H_3O^+	$HOCO^+$	H_2CO	C_3O	CH_2CO	HCOOH	H_2COH^+	CH_3OH	C_5O
HC_2CHO	CH_3CHO	c-CH_2OCH_2	CH_2CHOH	CH_3COOH	$HCOOCH_3$	C_2H_5OH	$H_2COHCHO$	CH_3OCH_3
CH_3CH_2OH	$(CH_3)_2CO$	$CH_3OC_2H_5$	$(C_2H_5)_2O$	$(CH_2OH)_2$				

Hydrogen + nitrogen + carbon containing molecules

NH	CN	N_2	HCN	HNC	N_2H^+	NH_2	NH_3	$HCNH^+$
H_2CN	HCCN	C_3N	CH_2NH	HC_2CN	HC_2NC	HNCCC	NH_2CN	CH_2CN
CH_3CN	CH_3NC	HC_3NH^+	CH_3NH_2	C_5N	CH_2CHCN	HC_4CN	CH_3C_2CN	CH_3CH_2CN
HC_6CN	HC_7CN	$HC_{10}CN$						

Hydrogen + nitrogen + oxygen + carbon containing molecules

NO	HNO	N_2O	HNCO	NH_2CHO

Other species

CS	SO	SO^+	SN	*SiC	SiN	SiO	SiS	HCl
HF	*CP	*NaCl	*AlCl	*KCl	*AlF	PN	C_2S	SO_2
OCS	HCS^+	H_2S	c-SiC_2	H_2CS	HNCS	C_3S	*$HSiC_2$?	SiC_3
*SiH_4	*SiC_4	C_5S	CH_3SH	*NaCN	*MgCN	*MgNC	SiCN	c-CH_2SCH_2

-

C_6H^-.....

Motivations

- H_3^+ is the cornerstone of ion-molecule reactions in the interstellar medium (ISM)
- Simple chemistry allows for the inference of various physical parameters (density, temperature, ionization rate, cloud size)

Table 1 Classification of Interstellar Cloud Types

	Diffuse Atomic	Diffuse Molecular	Translucent	Dense Molecular
Defining Characteristic	$f^n_{H_2} < 0.1$	$f^n_{H_2} > 0.1$ $f^n_{C+} > 0.5$	$f^n_{C+} < 0.5$ $f^n_{CO} < 0.9$	$f^n_{CO} > 0.9$
A_V (min.)	0	~0.2	~1–2	~5–10
Typ. n_H (cm^{-3})	10–100	100–500	500–5000?	$>10^4$
Typ. T (K)	30–100	30–100	15–50?	10–50
Observational Techniques	UV/Vis H I 21-cm	UV/Vis IR abs mm abs	Vis (UV?) IR abs mm abs/em	IR abs mm em

The Orion molecular clouds

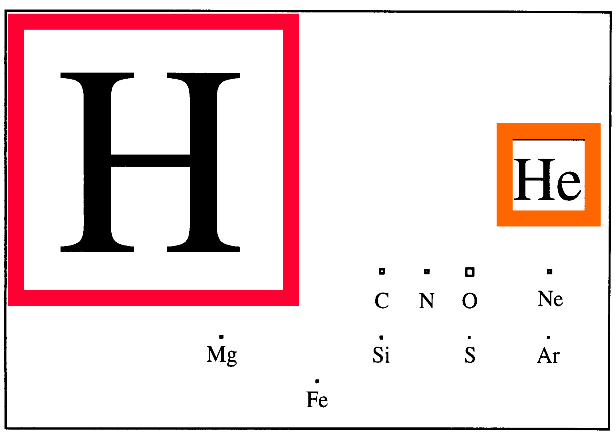

Figure 1. "The Astronomer's Periodic Table". The area of each element is proportional to its cosmic abundance.

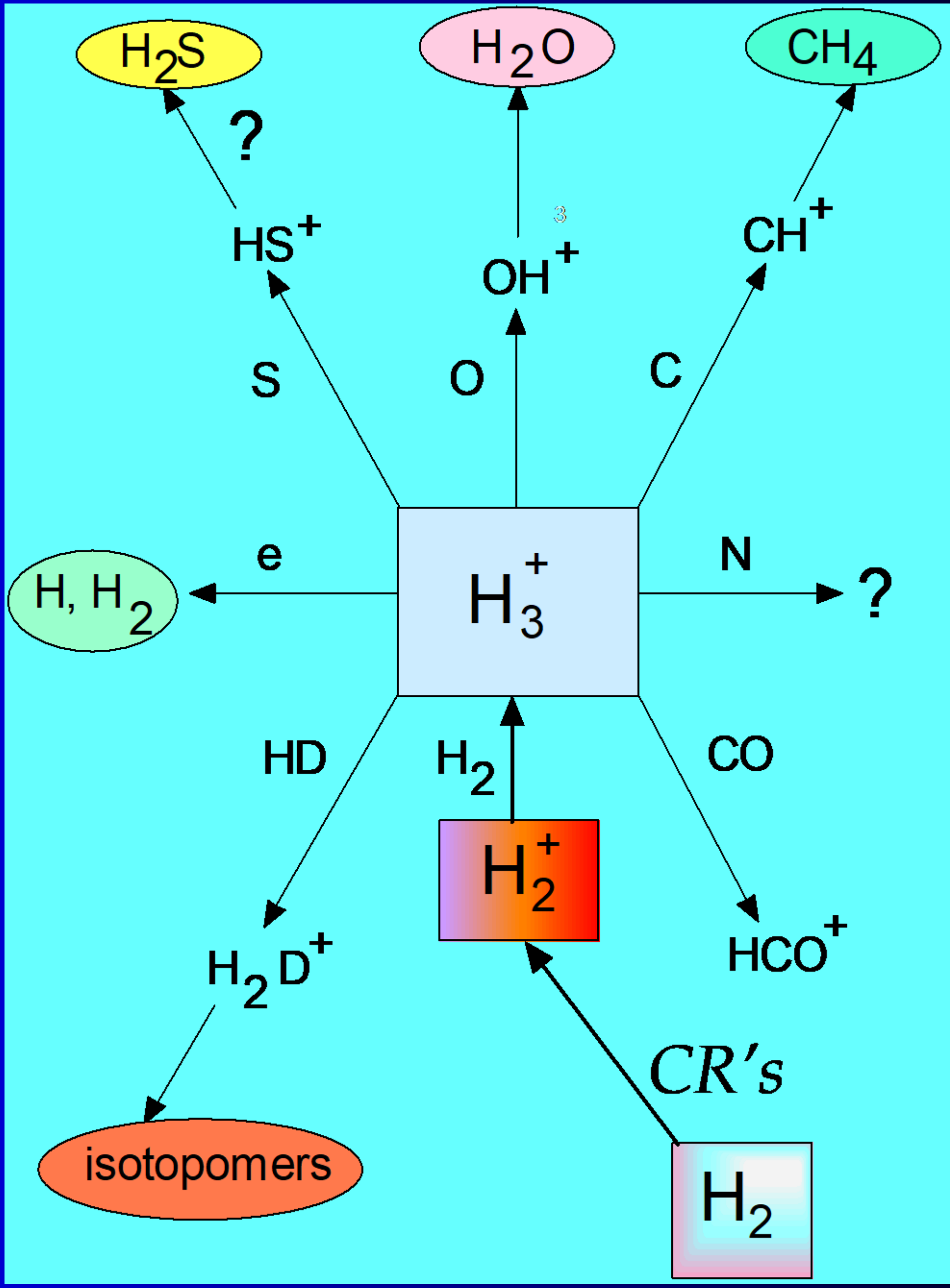

History of H_3^+

J. J. Thomson 1912

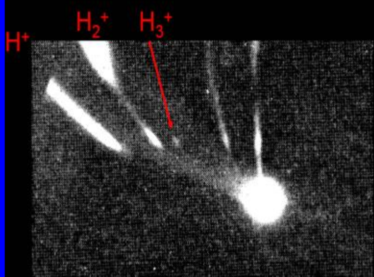

Existence of H_3.—On several plates taken when the discharge-tube contains hydrogen, the existence of a primary line for which $m/e = 3$ has been detected. There can, I think, be little doubt that this line is due to H_3 The existence of this substance is interesting from a chemical point of view, as it is not possible to reconcile its existence with the ordinary conceptions about valency, if hydrogen is regarded as always monovalent. The polymeric modification of hydrogen seems to require special conditions for its formation, for it cannot be detected on many of the plates taken with hydrogen in the tube.

J. J. Thomson, Phil. Mag. 24, 209 (1912)

m=3

Arthur J. Dempster 1916

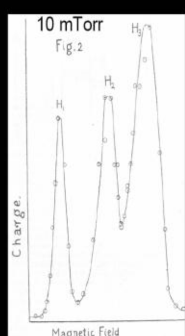

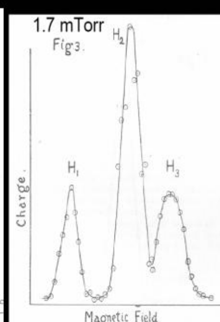

- Discovered ^{235}U
- Physics Prof. at U. Chicago
- Principal American authority on positive rays

$\rightarrow H_3^+$ formed in secondary reaction

A. J. Dempster, Phil. Mag. 31, 438 (1916)

$$H_2^+ + H_2 \rightarrow H_3^+ + H$$

1935 Charles A. Coulson

- First Ph.D. student of Lennard-Jones
- First ab initio calculation on a polyatomic molecule
- "It appears that the ion H_3^+ should exist in stable equilateral form with a nuclear distance about 0.85 Å, and that all excited levels are unstable."
- Prediction not accepted by Eyring, Hirschfelder, and others
- With advent of computers, prediction was confirmed (Christoffersen, Hagstrom, & Prosser 1964, Conroy 1964)

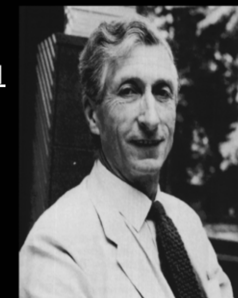

C. A. Coulson, Proc. Camb. Phil. Soc. 31, 244 (1935)

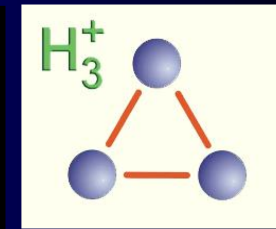

- No excited electronic state
- No dipole moment in ground state
  - $\rightarrow$ no pure rotational spectrum
- ν_1 symetric stretch - infrared inactive
- ν_2 vibration fundamental band feasible freq. ~2700 cm^{-1}

Intensive laboratory search for H_3^+ spectra

1912 1920 1930 ……. 1970 1980

H_3^+ in Interstellar space

Interstellar H_3^+

1961

ON THE POSSIBLE OCCURRENCE OF H_3^+ IN INTERSTELLAR SPACE

The possibilities for detection of the molecular ion H_2^+ by radio-astronomical techniques have recently received considerable attention, and theoretical predictions of the spectrum have been made by Mizushima (1961) and by Burke (1961). Recent work on ion-molecule reactions indicates that the molecular ion H_3^+ may also be expected in interstellar space. In fact, with the presence of quantities of molecular hydrogen, H_2^+ will react to form H_3^+.

Formation of H_3^+ through the reaction $H_2^+ + H_2 \rightarrow H_3^+$ has been observed independently by Stevenson and Schissler (1958) and by Barnes, Martin, and McDaniel (1961). The cross-section for this reaction has been found to have a remarkably large value of the order of 10^{-14} cm^2 at normal thermal energies. This is much greater than the gas-kinetic cross-section for neutral hydrogen molecules. The cross-section for H_3^+ formation by this reaction varies inversely with the relative velocity of the H_2^+ ion and the hydrogen molecule (Stevenson and Schissler 1958; Lampe and Field 1959). The experimental work of Barnes, Martin, and McDaniel furthermore shows that H_3^+ ions persist over very many subsequent collisions with hydrogen molecules. The H_3^+ ion is stable against spontaneous dissociation. Its binding energy of 4.18 ev (Varney 1960) exceeds that of H_2^+ (2.65 ev), so the formation reaction is exoergic (Hirschfelder, Curtiss, and Bird 1954).

Thus it may be expected that H_2^+ will be converted to H_3^+ upon encounter with a hydrgoen molecule, and the population of H_2^+ will be very strongly influenced by the density of neutral molecular hydrogen. It now appears desirable to consider the possibilities for detecting H_3^+ because this molecular ion may be present under some circumstances to the virtual exclusion of H_2^+.

D. W. MARTIN
E. W. MCDANIEL
M. L. MEEKS

June 13, 1961
GEORGIA INSTITUTE OF TECHNOLOGY
ATLANTA, GEORGIA

Martin, McDaniel, & Meeks, Astrophys. J. 134, 1012 (1961)

H_3^+ in Interstellar space

Interstellar Chemistry

1973

Another important subclass of reactions are those involving H_3^+. This ion is produced by the well-studied reaction

$$4.\quad H_2 + H_2^+ \rightarrow H_3^+ + H\,,$$

and then reacts with many neutral species according to the general formula

$$H_3^+ + X \rightarrow XH^+ + H_2\,, \qquad (4)$$

where X = CO, N_2, H_2O, NH_3, etc. These reactions have been studied by Burt *et al.*

E. Herbst & W. Klemperer, Astrophys. J. 185, 505 (1973)

also: W. D. Watson Astrophys. J. 183, L17 (1973)

- H_3^+ "universal protonator"
  - $H_3^+ + O \rightarrow H_2 + OH^+$
  - $OH^+ + H_2 \rightarrow H + H_2O^+$
  - $H_2O^+ + H_2 \rightarrow H + H_3O^+$
  - $H_3O^+ + e^- \rightarrow H_2O + H$
- Origin of Earth's water (?)

Search for H_3^+ in laboratory

Oka's Search for H_3^+

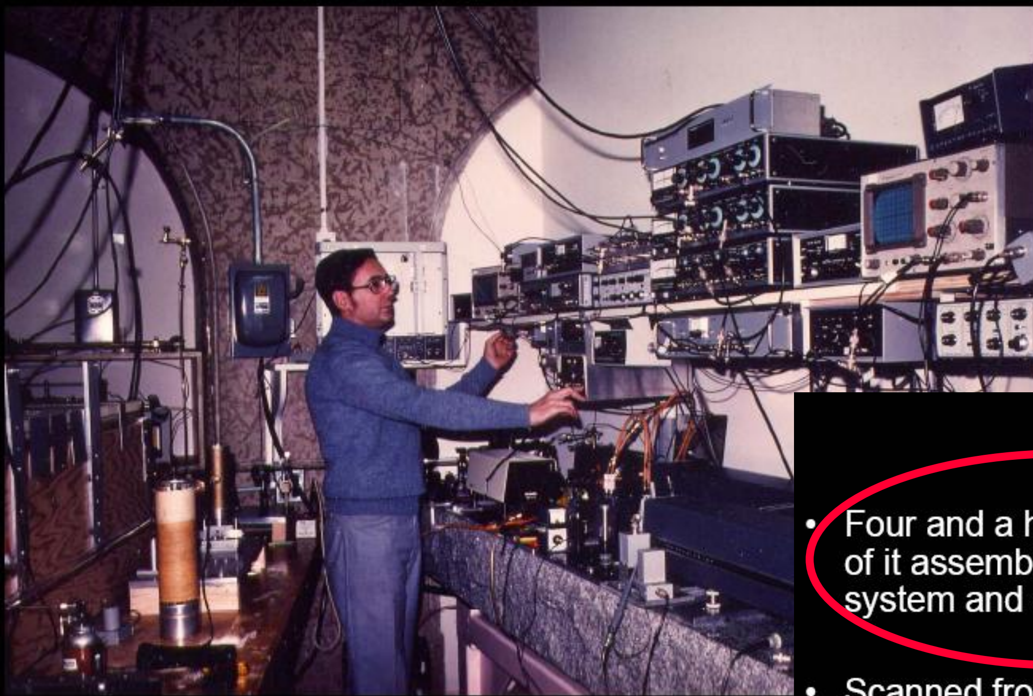

Positive Column Discharge

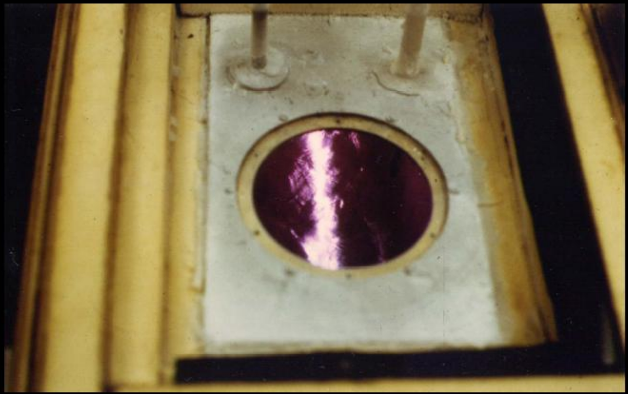

Every morning, he transferred six 50 liter cans of liquid nitrogen to the laboratory!

The Long Search

- Four and a half years. Much of it assembling the DF system and discharge cell.
- Scanned from:
  - 6/12-8/3 (1978)
  - 12/18-1/26 (1978-79)
  - 4/24-12/18 (1980)
- R(1,0) April 25, 1980.
  - Oka and Allen Karabonik in lab
  - Keiko came in at 10 pm
- Watson assigned it overnight

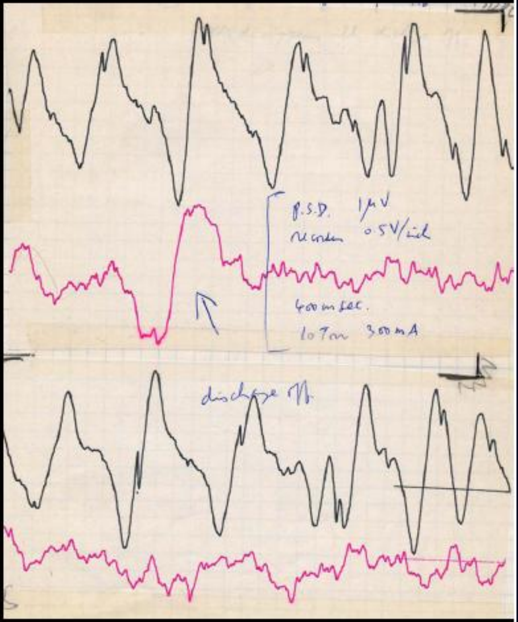

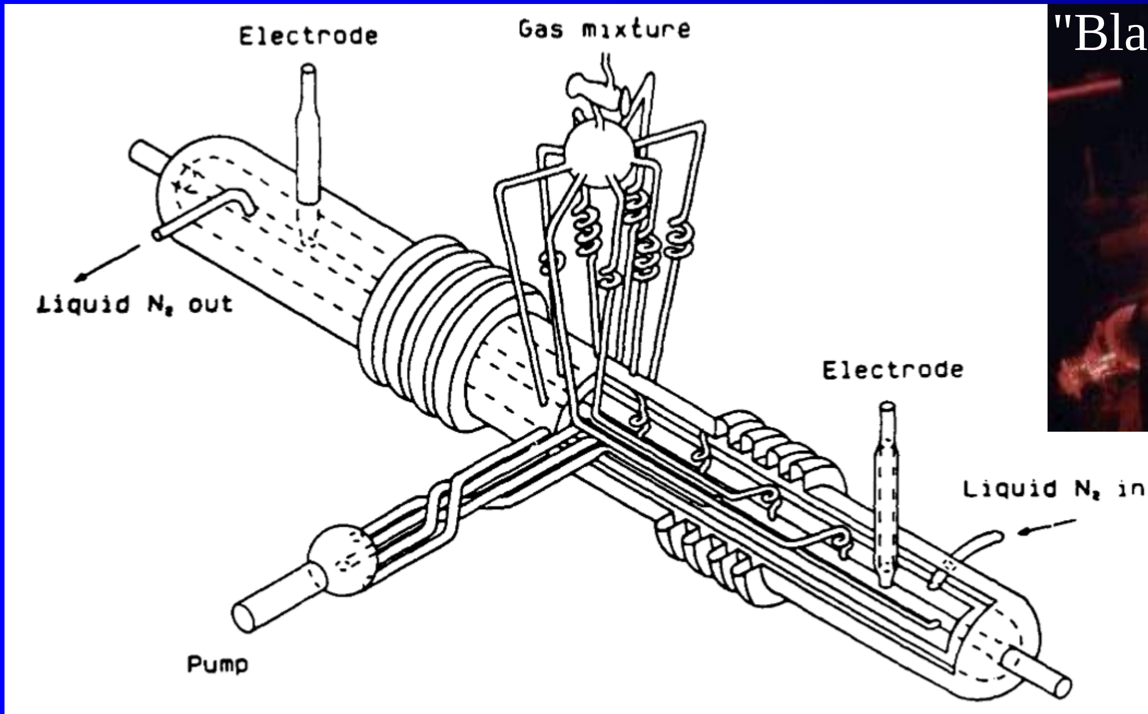

Fig. 8. The multiple inlet-outlet liquid nitrogen cooled plasma tube (nicknamed "Black Widow").

Aastrophysical – Observations of H_3^+(v=0)

1912 .. 1916 … 1935 ……….. 1980

1980 - Laboratory

T. Oka -IR Spectroscopy Observation of H_3^+

Oka, T. 1980 *Phys. Rev. Lett* 45, 531.

"Black Widow"

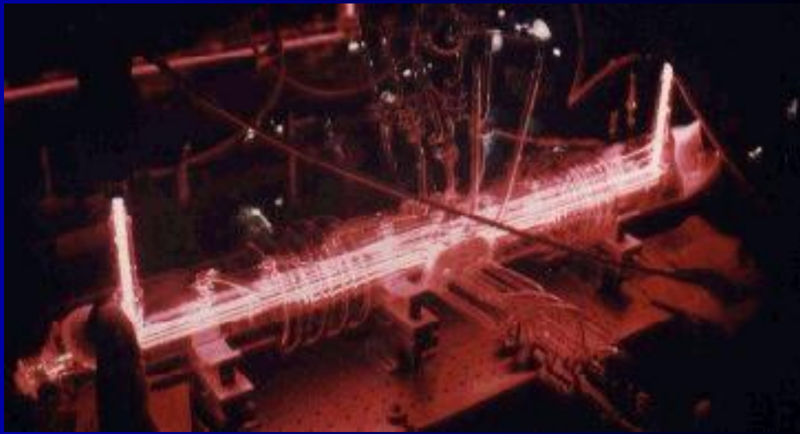

NATURE | VOL 422 | 3 APRIL 2003

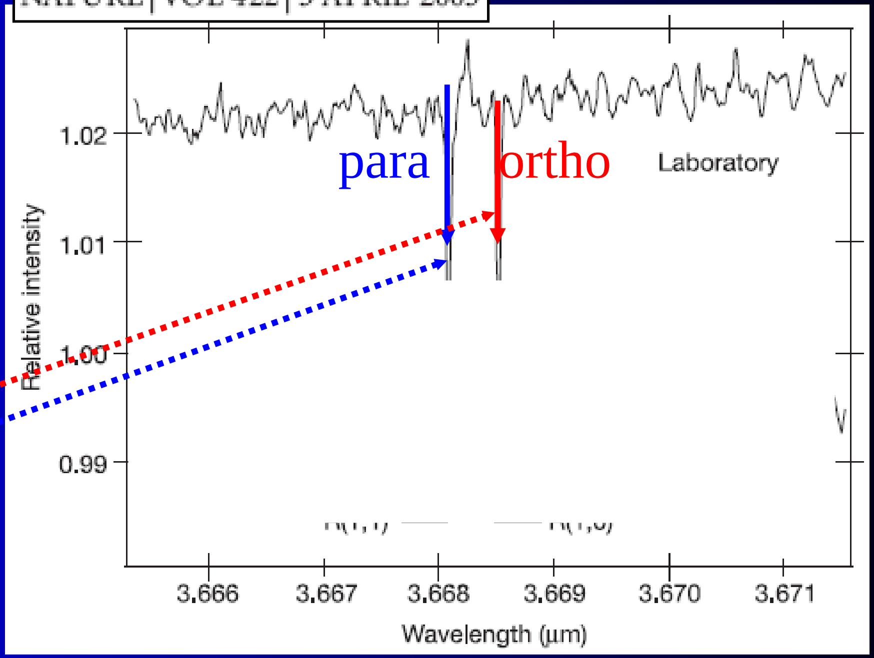

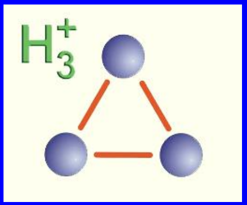

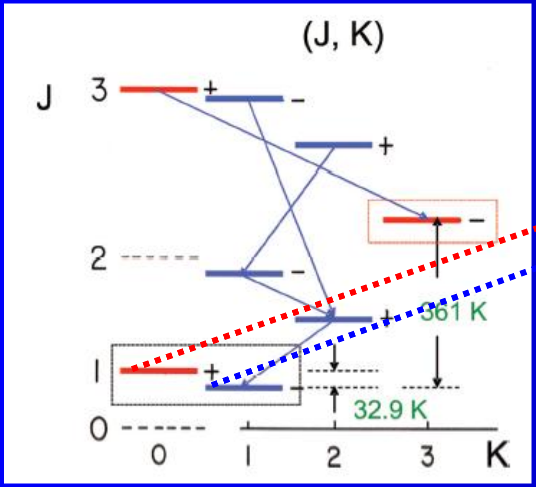

R(1,1)u originates from the lowest para level (J = 1, K = 1), while R(1,0) comes from the lowest ortho level (J = 1,K = 0). Note that the (J = K = 0) level is forbidden by the Pauli principle.

Back to the Interstellar Search

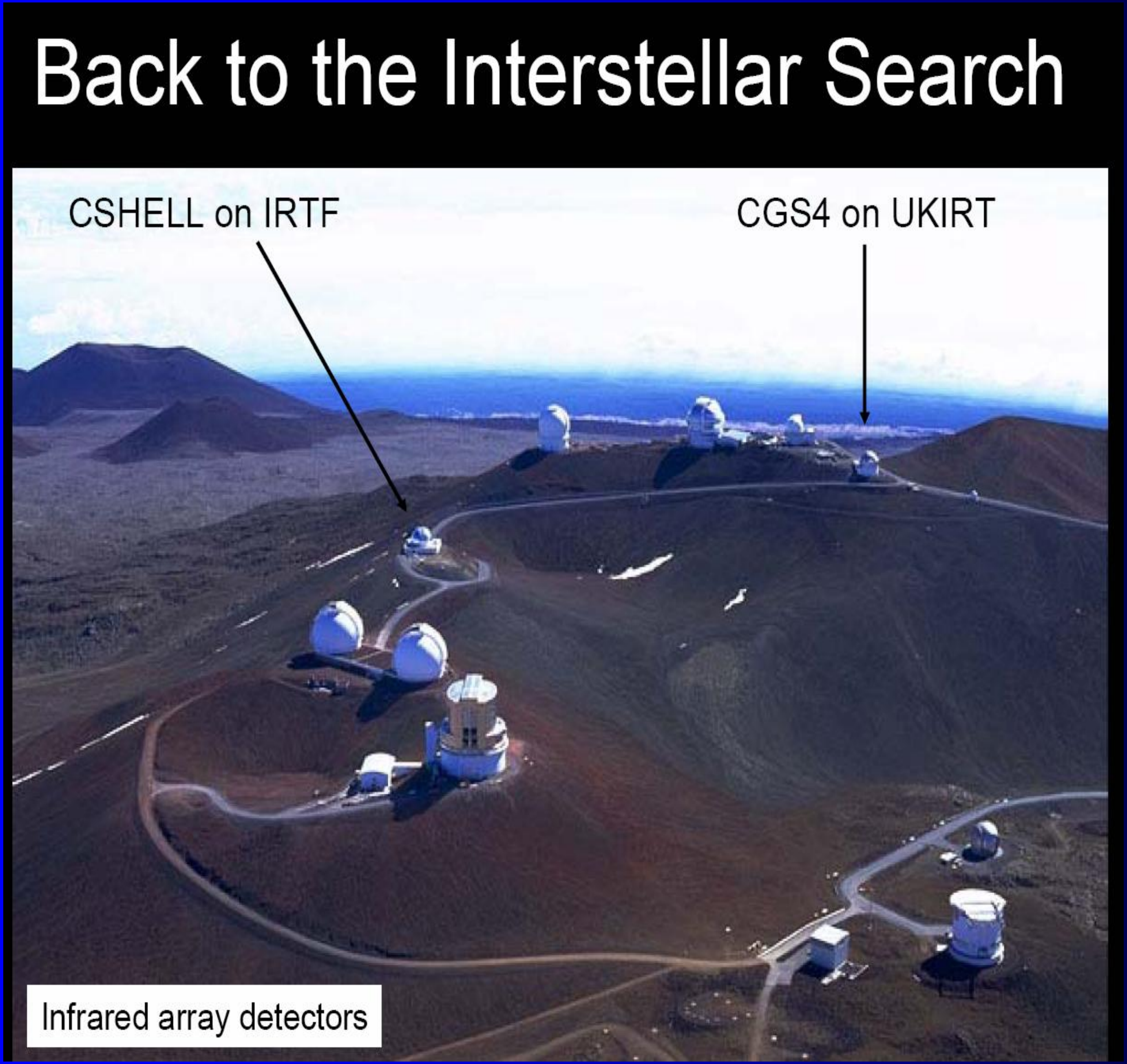

Environments with H_3^+

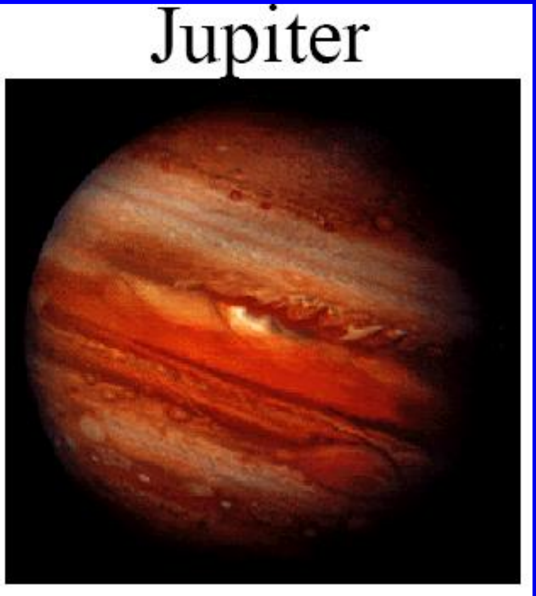

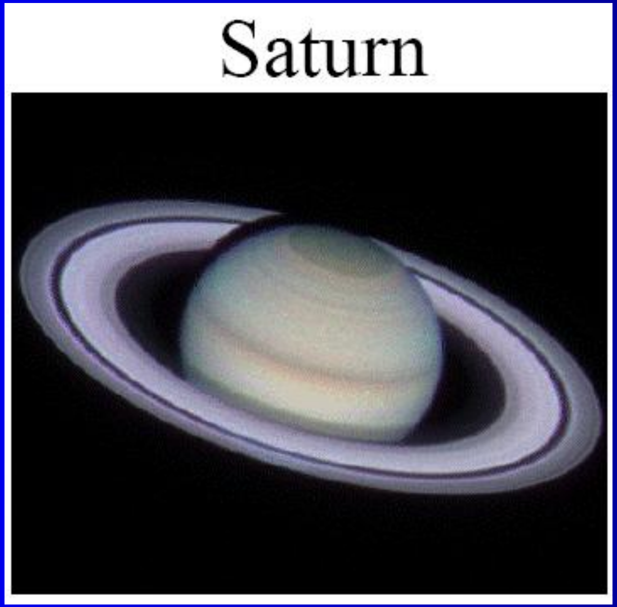

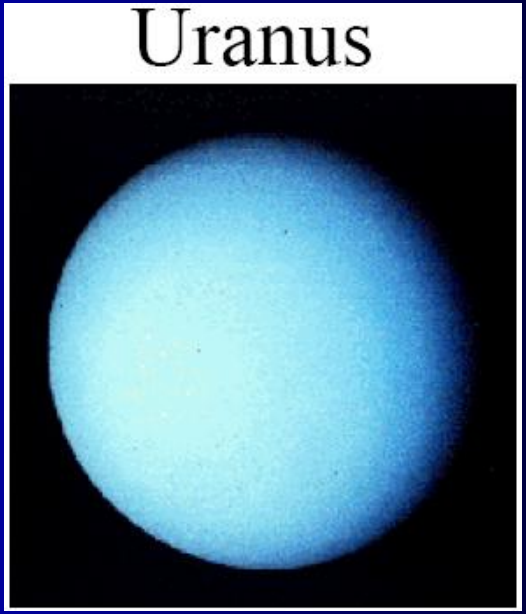

Observation of H_3^+: **1987-1993**

Ionosphere of large planets:

Jupiter (1987), Saturn (1993), Uran(1993)

Search for H_3^+ - Interstellar space

First detection!

LETTERS TO NATURE **1996**

Detection of H_3^+ in interstellar space

T. R. Geballe* & T. Oka†

* Joint Astronomy Centre, University Park, Hilo, Hawaii 96720, USA
† Department of Astronomy and Astrophysics, Department of Chemistry and the Enrico Fermi Institute, The University of Chicago, Chicago, Illinois 60637-1403, USA

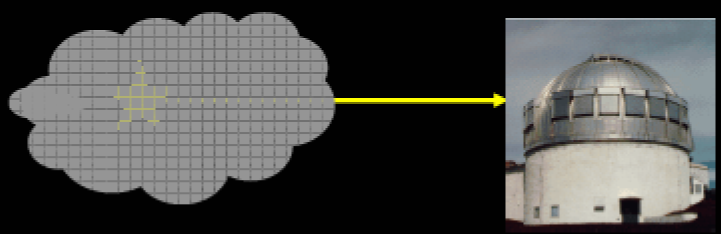

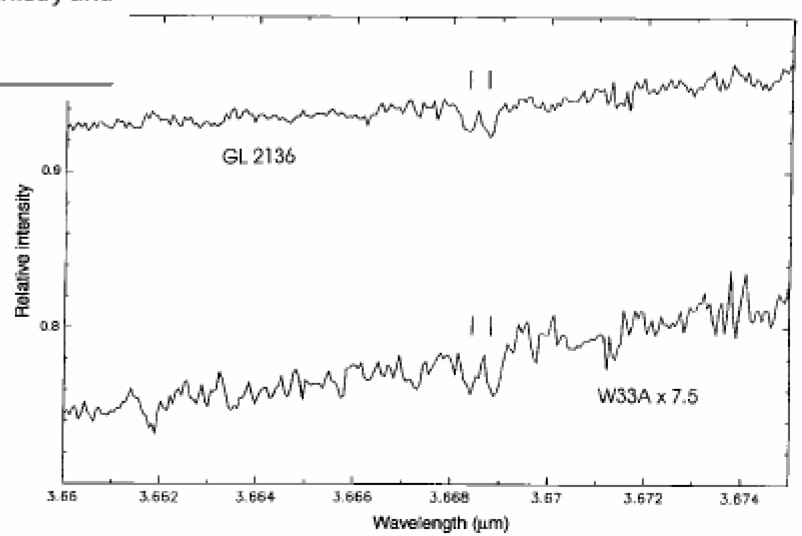

T. R. Geballe & T. Oka, Nature 384, 334 (1996)

Search for H_3^+ - Interstellar space

Confirmed by Doppler Shift

1996

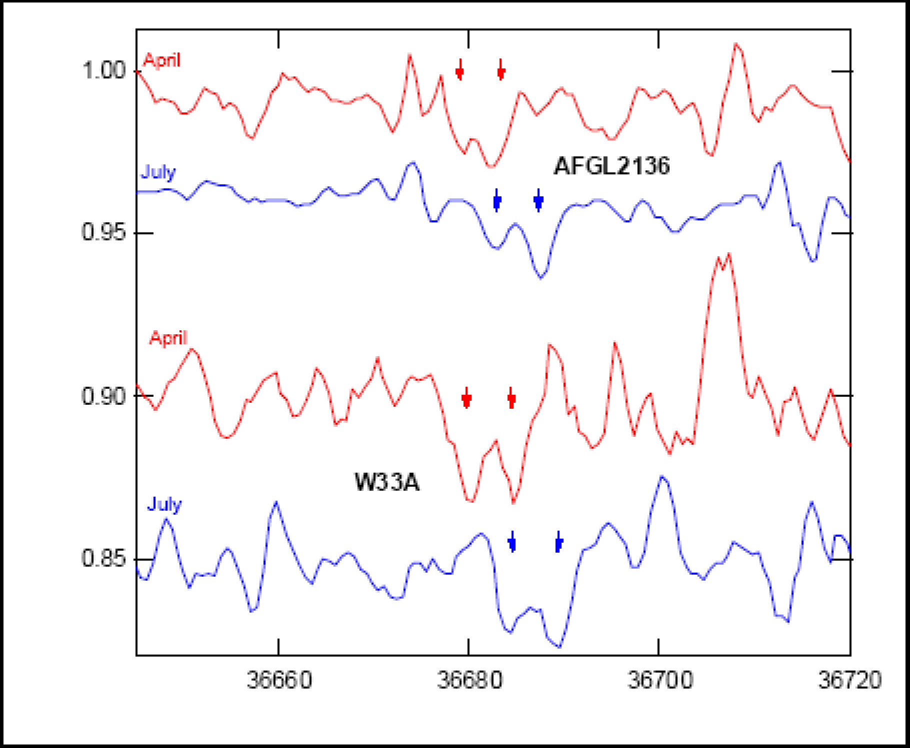

reprocessed
↓
Doppler shift
confirms
interstellar
origin

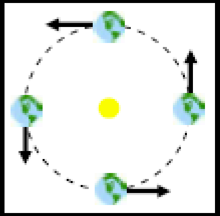

B. J. McCall, T. R. Geballe, K. H. Hinkle & T. Oka,
Astrophys. J. 522, 338 (1999) **1996**

Conditions in ISM

T. R. Geballe & T. Oka
Nature 384, 334 (1996)

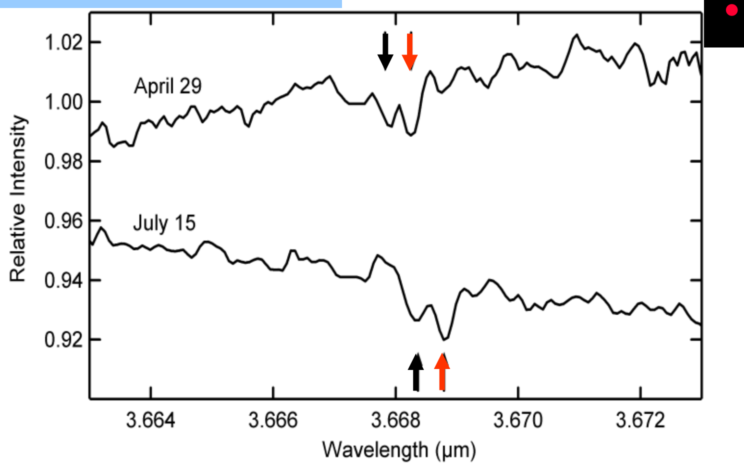

$N_{para} = 4.0(9) \times 10^{14}\ cm^{-2}$

$N_{ortho} = 3.0(6) \times 10^{14}\ cm^{-2}$ (ΔE~32.9K)

Molecular Cloud GL2136.
The first detection of interstellar H_3^+
CGS4 spectrometer at UKIRT

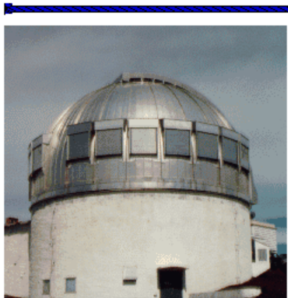

United Kingdom Infrared Telescope

(UKIRT)

Dark Clouds:

- **T ~ 10K**
- **H_2 density ~ $10^4 cm^{-3}$**

The Orion molecular clouds

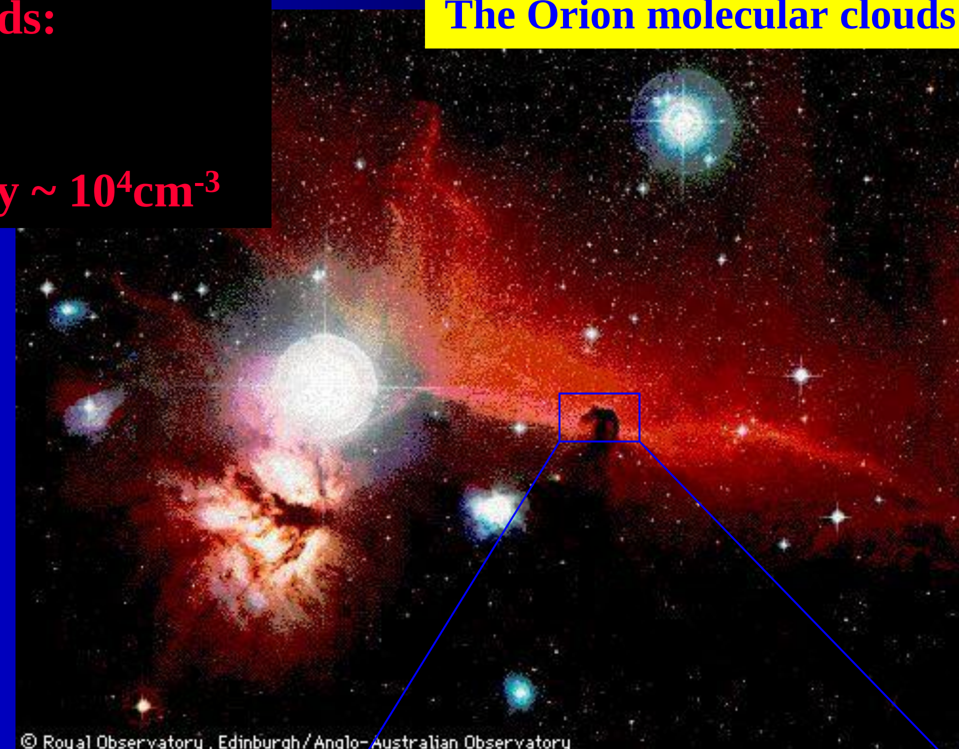

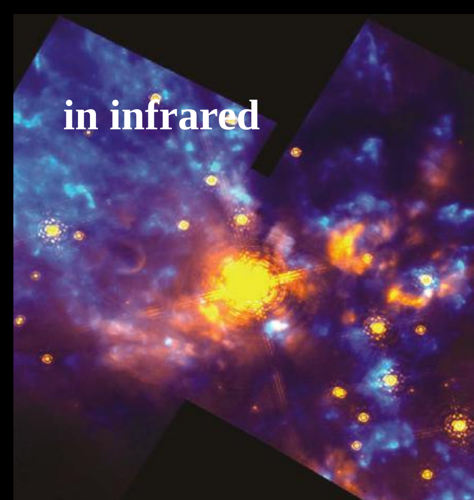

Aastrophysical – Observations OF H_3^+(v=0)

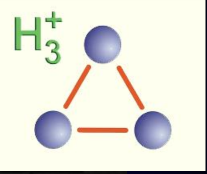

1980 - Laboratory

T. Oka -IR Spectroscopy Observation of H_3^+

Oka, T. 1980 *Phys. Rev. Lett* 45, 531.

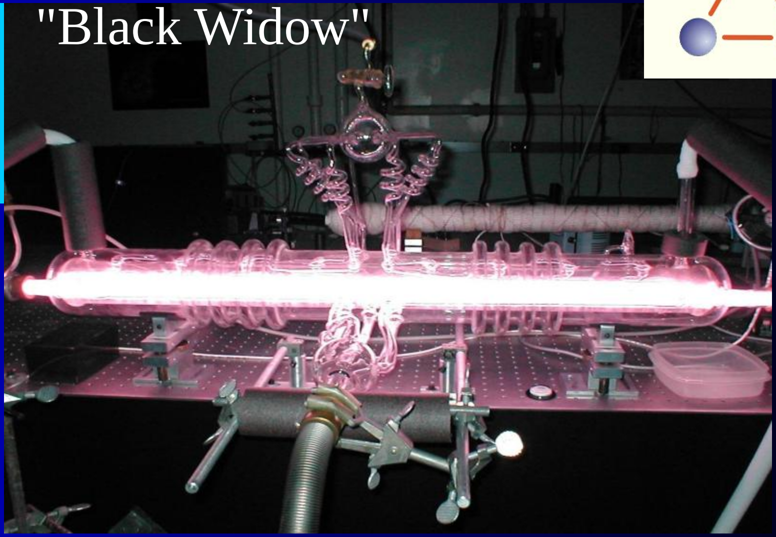

1987 -2006; Observation of H_3^+:

Supernova 1987A

Interstellar clouds (1998….)

Centre of Galaxy (1999)

Ionosphere of large planets:

Jupiter (1987), Saturn (1993), Uran(1993)

Geballe, T. R. & Oka, T. 1996 *Nature* 384, 334.

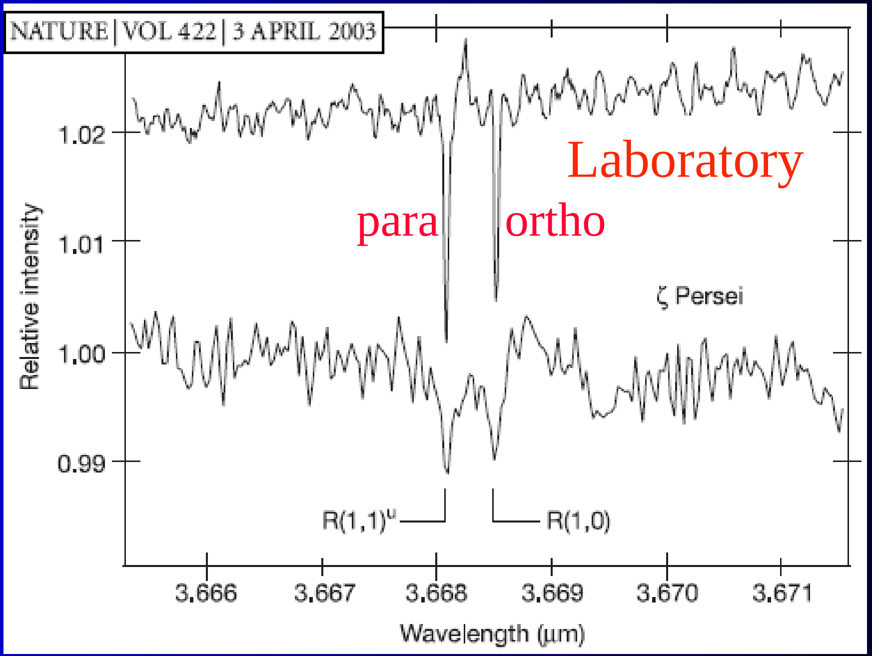

Jupiter

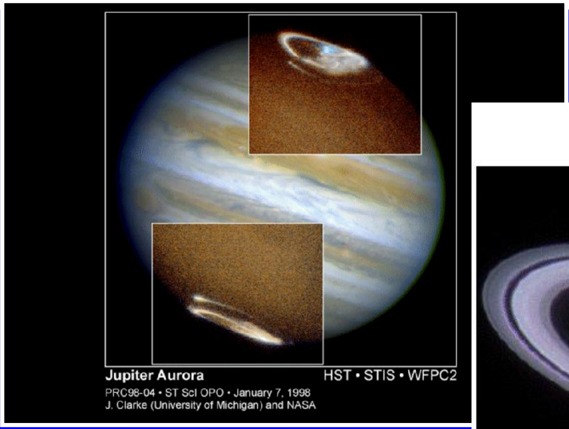

Saturn

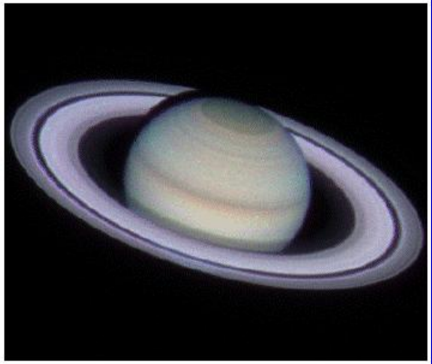

R(1,1)u originates from the lowest para level (J = 1, K = 1), while R(1,0) comes from the lowest ortho level (J = 1,K = 0). Note that the (J = K = 0) level is forbidden by the Pauli principle.

Environments with H3+

Jupiter

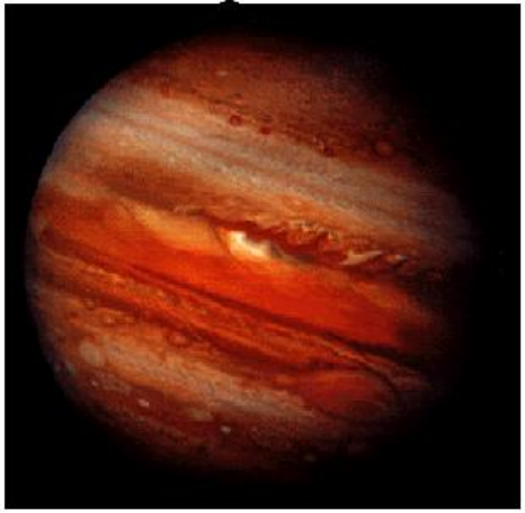

Saturn

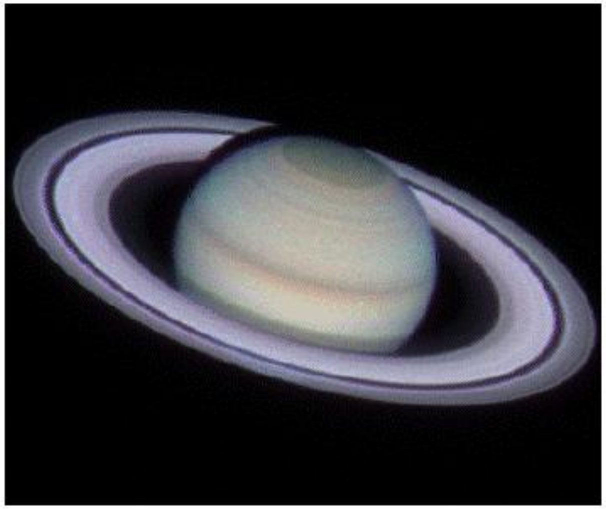

Uranus

Dense Clouds

Barnard 68 (João Alves)

Diffuse Clouds

Cygnus OB2 (POSS)

Galactic Center

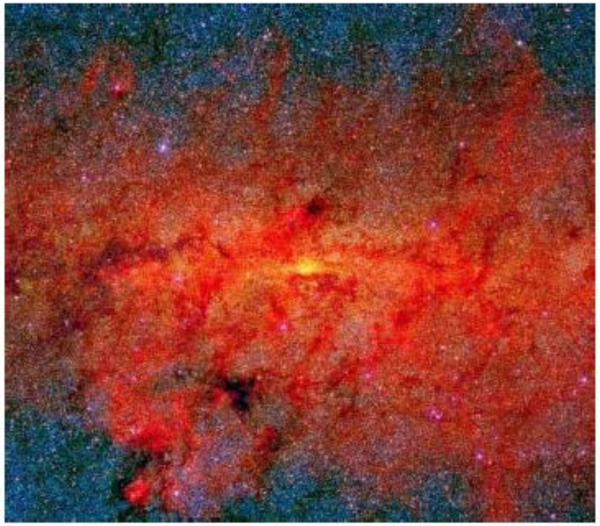

Galactic Center (2MASS/MSX)

Balance in ISM

Cosmic-ray ionisation rate $\gamma \sim 3 \times 10^{-17} s^{-1}$

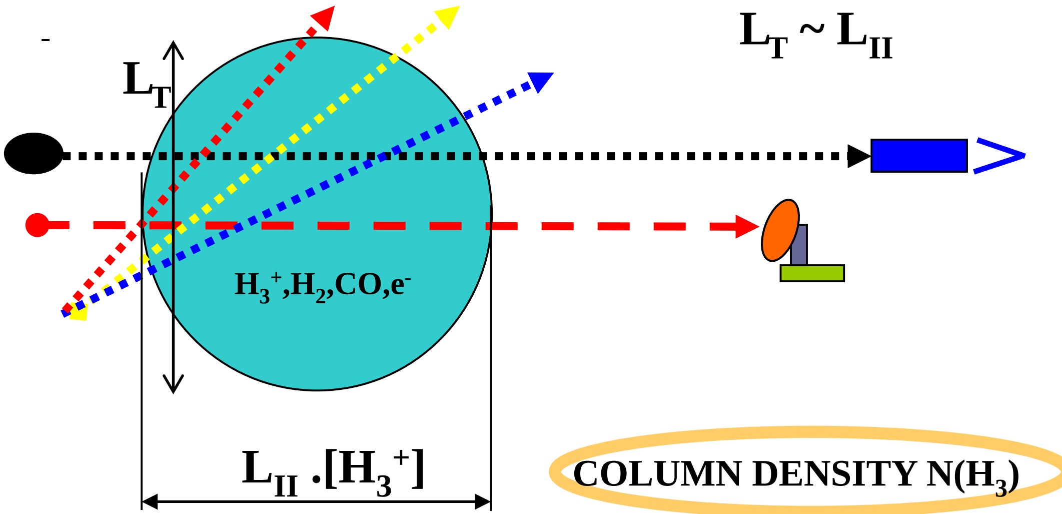

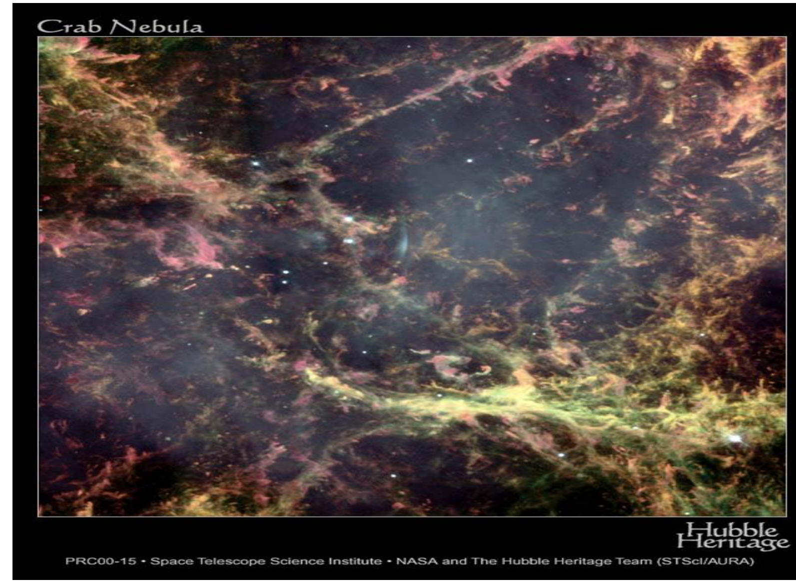

PRODUCTION: $H_2 \xrightarrow{h\nu} H_2^+ \xrightarrow{H_2} H_3^+$ $\quad d[H_3^+]/dt \sim \gamma.[H_2]$

a) DENSE CLOUDS: DESTRUCTION:

$H_3^+ + CO \rightarrow HCO^+ + H_2$

$k_{CO} = 2 \times 10^{-9} cm^3 s^{-1}$

$d[H_3^+]/dt \sim -k_{CO} x [H_3^+] x [CO]$

$[H_3^+] = \gamma / k_{CO} \,.\, [H_2]/[CO] =$ $\sim 1 \times 10^{-4} cm^{-3}$

~OK with observation

b) DIFFUSE CLOUDS: DESTRUCTION: $H_3^+ + e^-$

$d[H_3^+]/dt \sim -\alpha_{DR} [H_3^+][e^-]$

$[e^-] \sim [C]$

$\alpha_{DR} = 2 \times 10^{--7} cm^3 s^{-1} x (T/300)^{-0.65}$?

$[H_3^+] = \gamma / \alpha_{DR} \,.\, [H_2]/[C] =$ $\sim 1 \times 10^{-7} cm^{-3}$

~ NO with observation

Interstellar medium

@ 10-50K

92.1% of nucleons in the universe are protons
7.8% are helium nuclei !
0.1%……C,N,O,S,Si….

Cosmic abundance

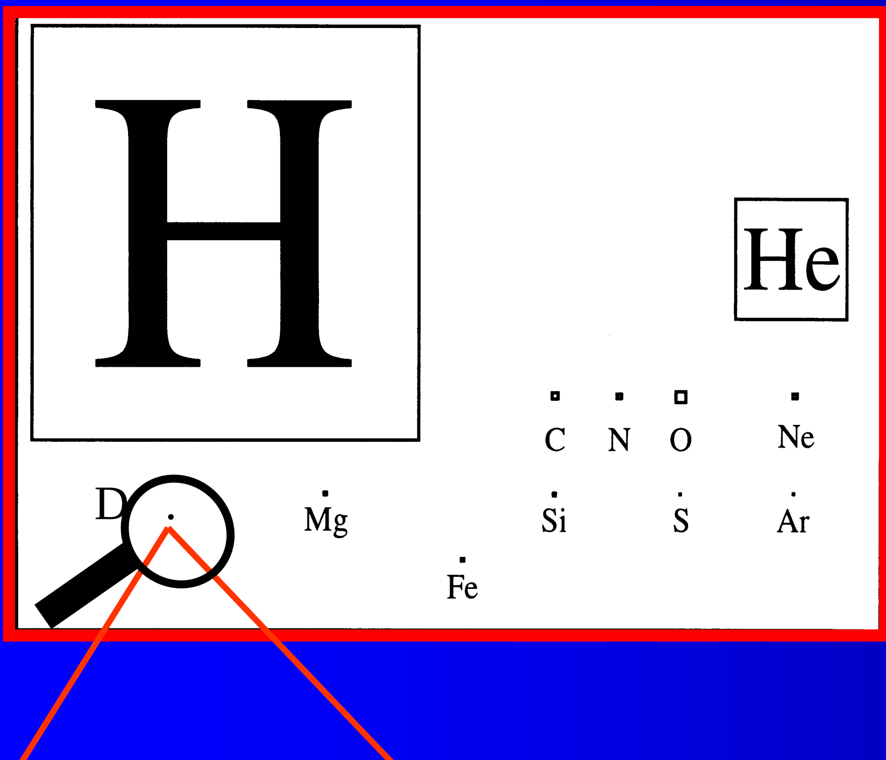

D/H ratio ~ 10^{-5}

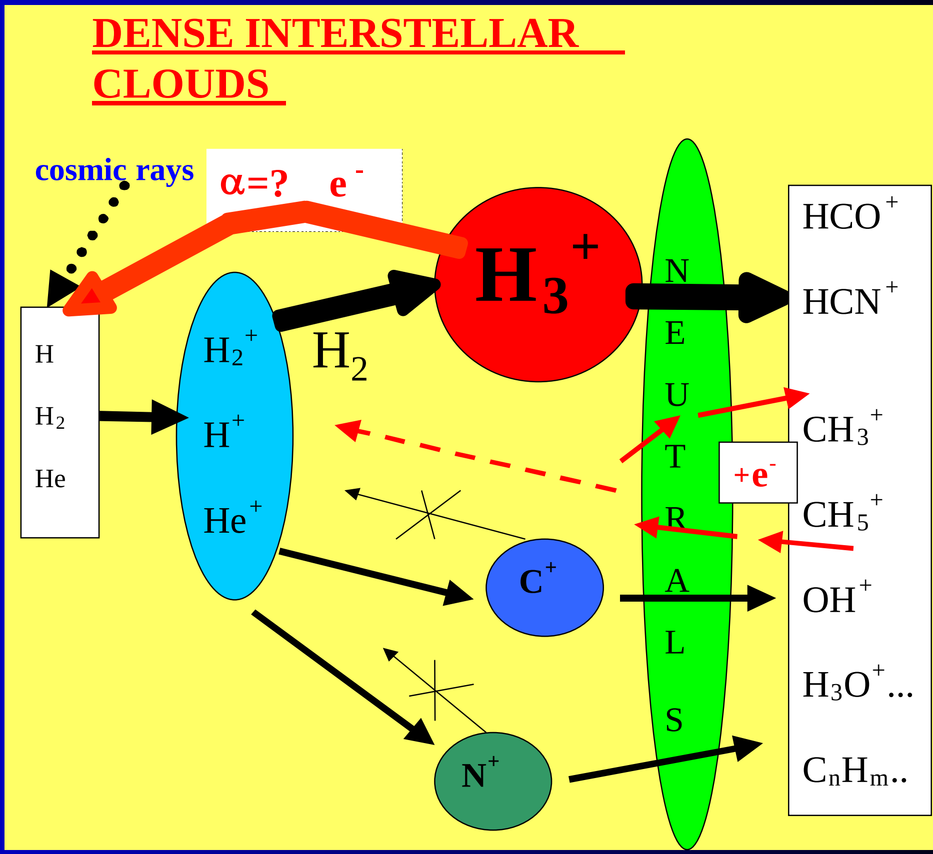

$$H_3^+ \ + \ e^- \xrightarrow{\alpha} neutral \ \ products$$

α (10 K) = ????

Emotional history of experiments

–“time evolution“ of $\alpha(H_3^+)$, $\alpha(D_3^+)$

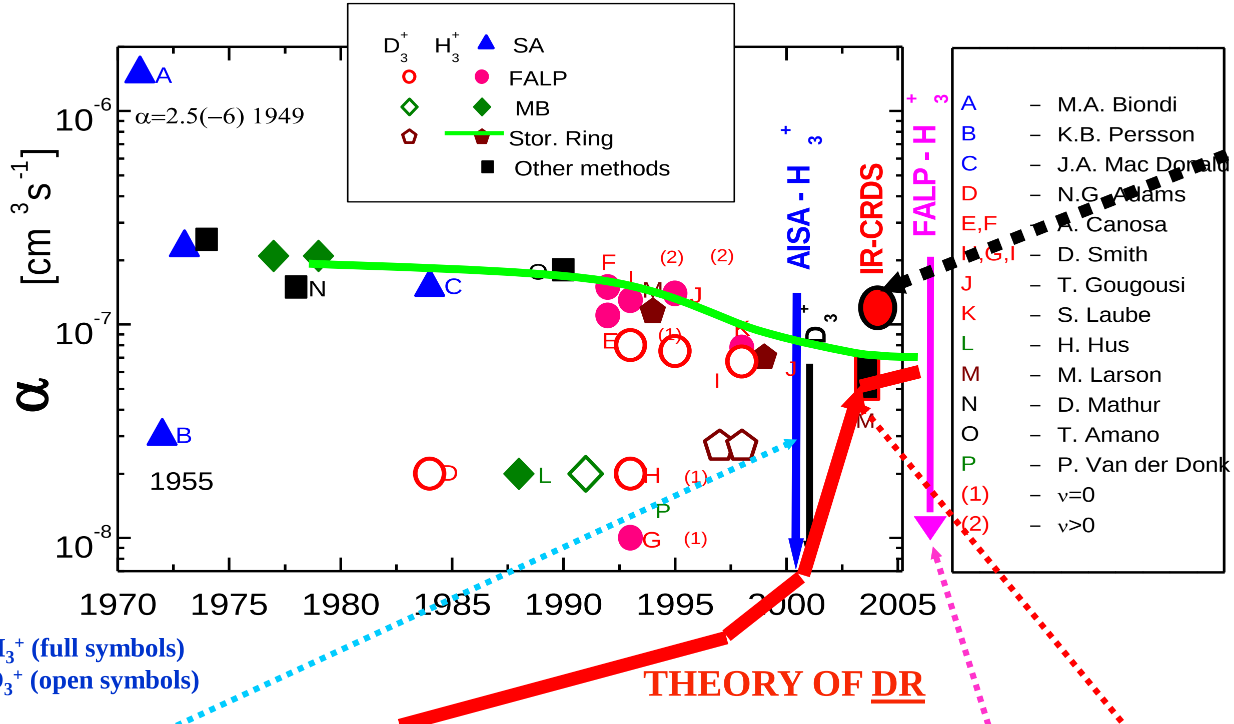

H_3^+ (full symbols)
D_3^+ (open symbols)

THEORY OF DR

CRDS

μw discharge cell

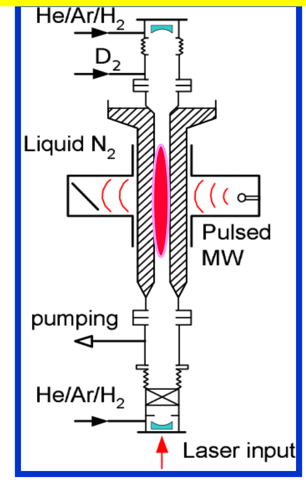

IR spectroscopy

PHYSICAL REVIEW A **68**, 012703 (2003)

Unified theoretical treatment of dissociative recombination of D_{3h} triatomic ions: Application to H_3^+ and D_3^+

Viatcheslav Kokoouline and Chris H. Greene

AISA

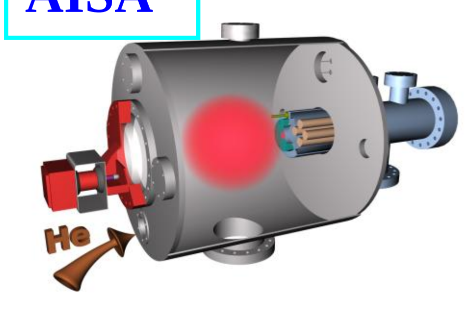

FALP

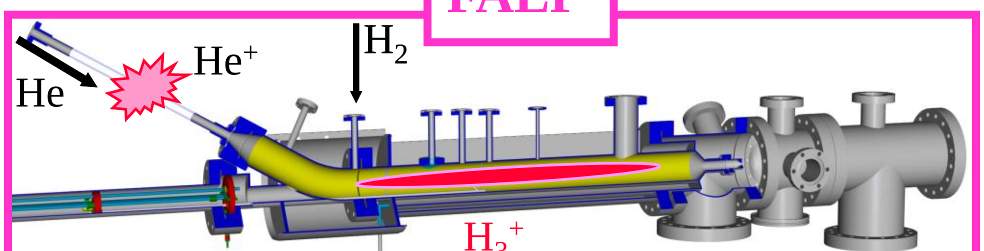

Interstellar medium, HD role

@ 10-50K

92.1% of nucleons in the universe are protons
7.8% are helium nuclei !
0.1%……C,N,O,S,Si….

Cosmic abundance

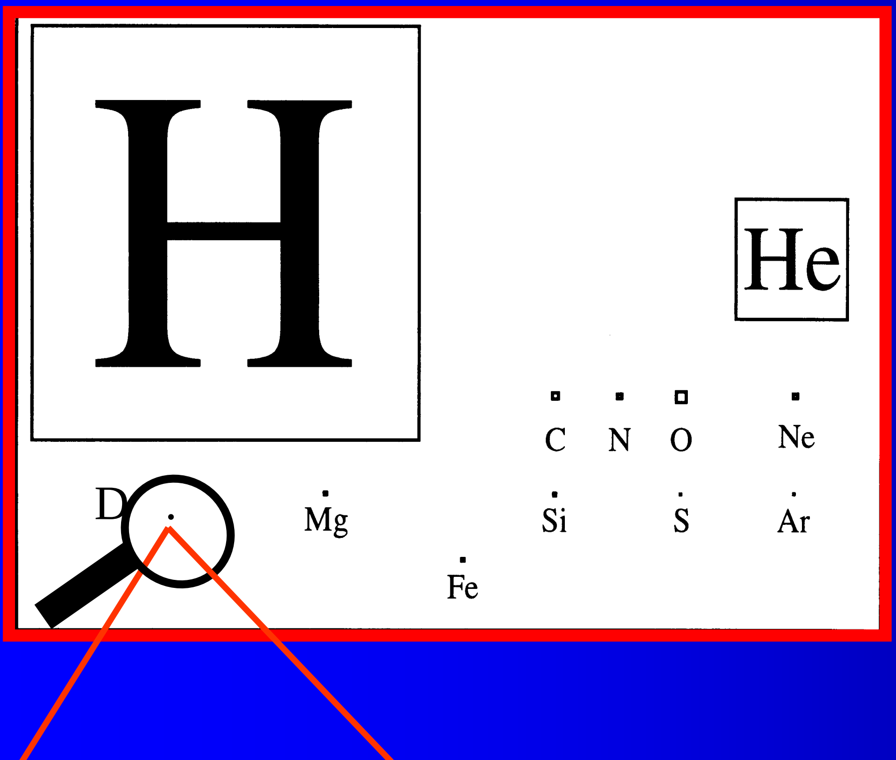

D/H ratio ~ 10^{-5}

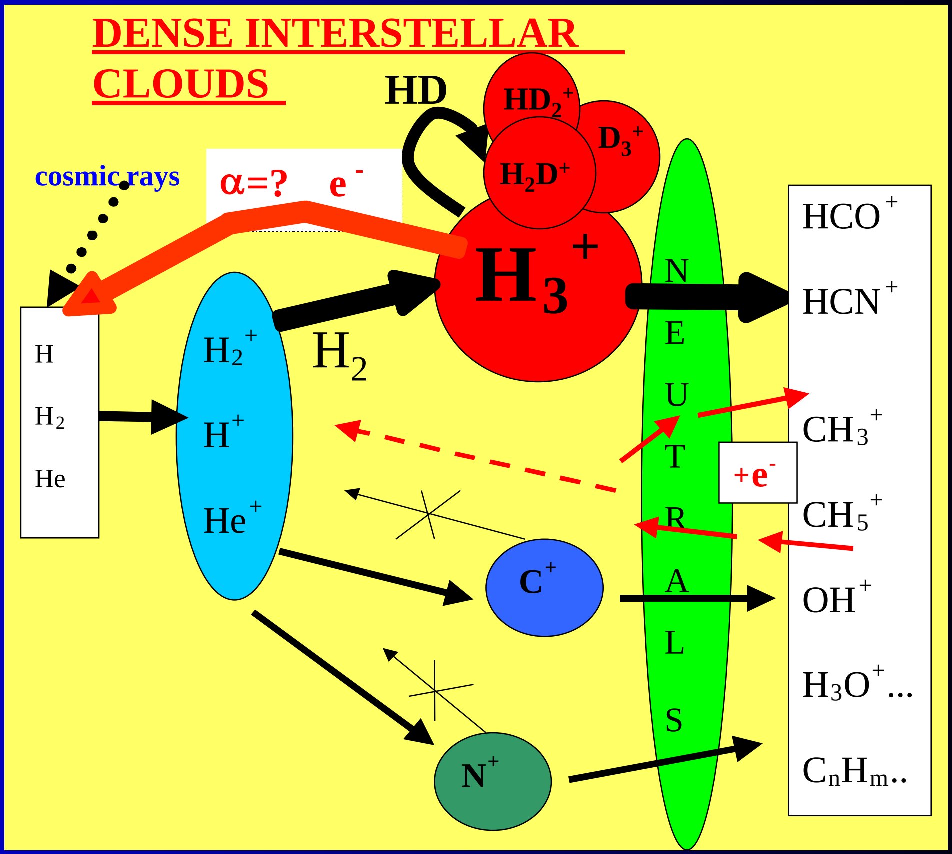

$$H_3^+ \quad + \quad e^- \quad \xrightarrow{\alpha} neutral\ \ products$$

α (10 K) = ????

k (10 K) = ????

$$H_3^+ \xrightarrow{HD} H_2D^+ \xrightarrow{HD} HD_2^+ \xrightarrow{HD} D_3^+$$

Laboratory astrophysics

H_2D^+ and HD_2^+ recombination with electrons at low temperature.


The Supernova of 1604


Johannes Kepler
Prague 1600-1612

H_3^+

para-H_3^+

ortho-H_3^+

H_2D^+

HD_2^+

D_3^+

Juraj Glosík

Charles University

Faculty of Mathematics and Physics

Radek Plašil
Petr Dohnal
Rainer Johnsen
Stepan Roucka
Ábel Kálosi

Oldrich Novotny
Viktoria Poterya
Andryj Pysanenko
Chris H. Greene
Ihor Korolov
Tomáš Kotrík
Petr Hlavenka
Jozef Varju
Petr Macko
Slava Kokoouline
Michal Hejduk
Peter Rubovič

1912 … 1936 … 1949 … 1990 … 2003 …2008 …2016…

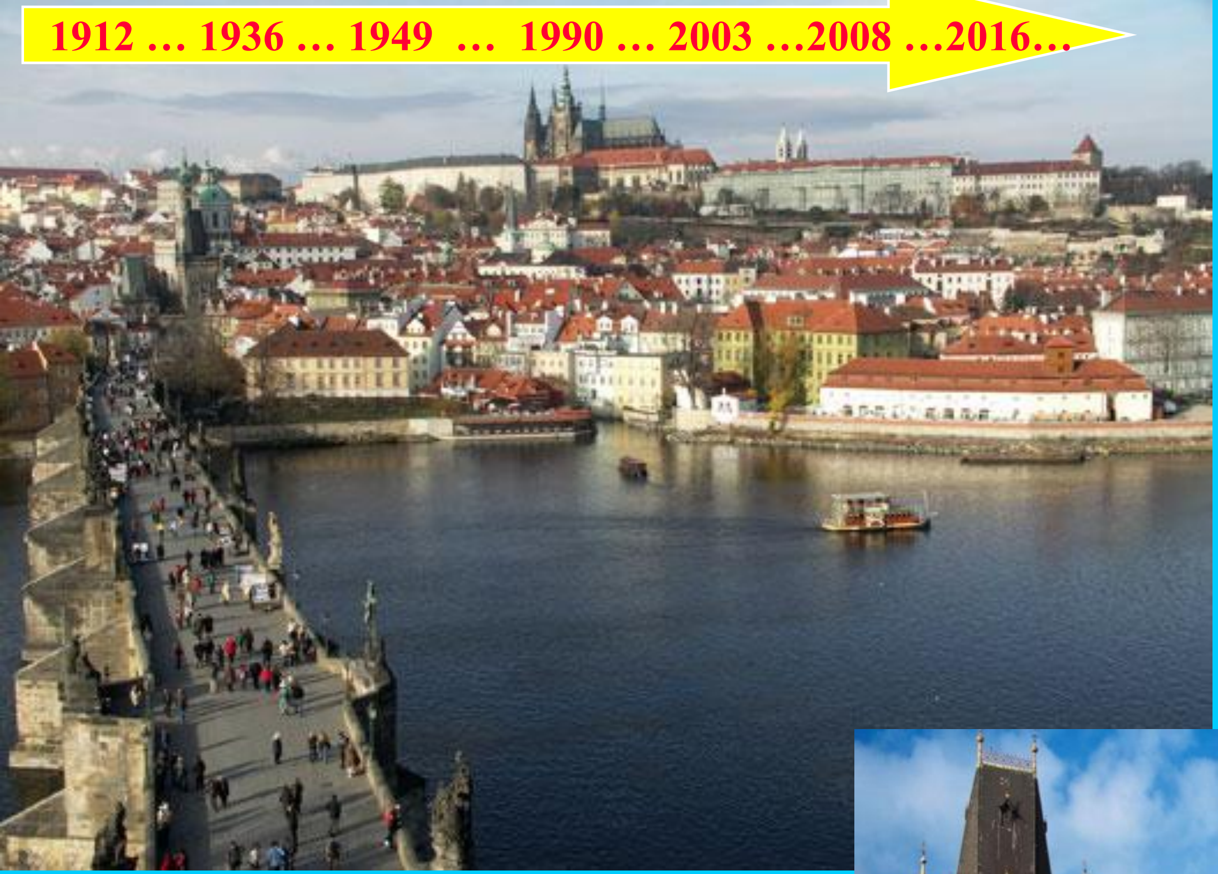

Charles University
Faculty of Mathematics and Physics

Juraj.glosik@mff.cuni.cz

1912 … 1936 … 1949 … 1990 … 2003 …2008 …2016…2023

04. 12. 2023

H_3^+ , H_2D^+, HD_2^+ D_3^+ are fundamental

A&A 494, 623–636 (2009)
DOI: 10.1051/0004-6361:200810587

Astronomy & Astrophysics

Chemical modeling of L183 (L134N): an estimate of the ortho/para H_2 ratio★

L. Pagani[1], C. Vastel[2], E. Hugo[3], V. Kokoouline[4], C. H. Greene[5], A. Bacmann[6], E. Bayet[7], C. Ceccarelli[6], R. Peng[8], and S. Schlemmer[3]

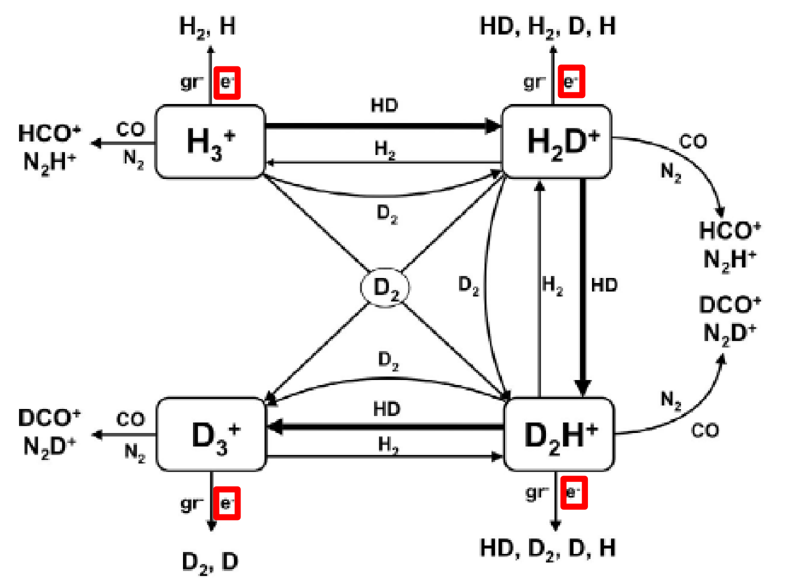

Fig. 4. Main reactions involved in the H_3^+ chemical network. When CO and N_2 are depleted, the reactions with bold arrows are dominant.

$$H_3^+ + e^- \xrightarrow{\alpha_{binH3}} \text{neutral products}$$

$$H_2D^+ + e^- \xrightarrow{\alpha_{binH2D}} \text{neutral products}$$

$$HD_2^+ + e^- \xrightarrow{\alpha_{binHD2}} \text{neutral products}$$

$$D_3^+ + e^- \xrightarrow{\alpha_{binD3}} \text{neutral products}$$

H_3^+ , H_2D^+, HD_2^+ D_3^+ are fundamental

PRL **102**, 023201 (2009) PHYSICAL REVIEW LETTERS

2009 Jahn-Teller Interactions in the Dissociative Recombination of H_3^+

Ch. Jungen[1,*] and S. T. Pratt[2]

A&A 494, 623–636 (2009)
DOI: 10.1051/0004-6361:200810587
© ESO 2009
Astronomy & Astrophysics

2009

Chemical modeling of L183 (L134N): an estimate of the ortho/para H_2 ratio*

L. Pagani[1], C. Vastel[2], E. Hugo[3], V. Kokoouline[4], C. H. Greene[5], A. Bacmann[6], E. Bayet[7], C. Ceccarelli[6], R. Peng[8], and S. Schlemmer[3]

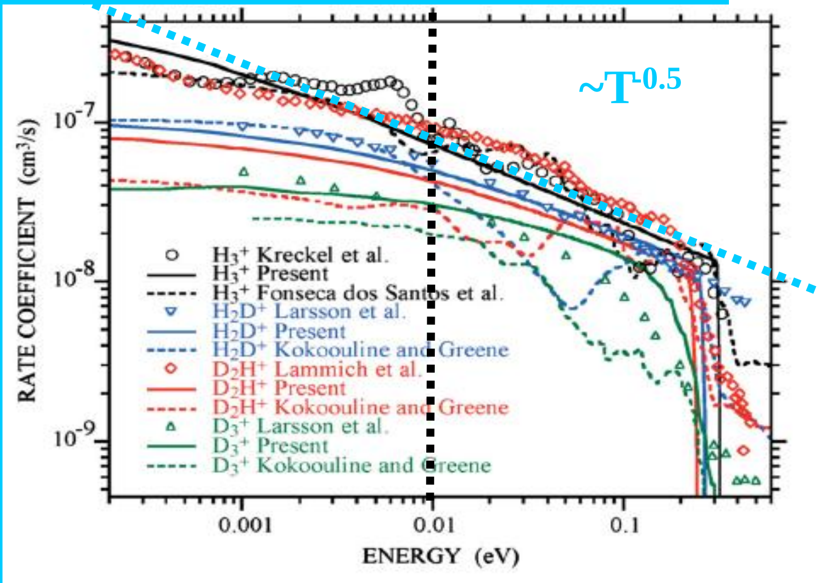

FIG. 3 (color). The DR rate coefficient of an electron and H_3^+, H_2D^+, D_2H^+, and D_3^+ as a function of collision energy. H_3^+

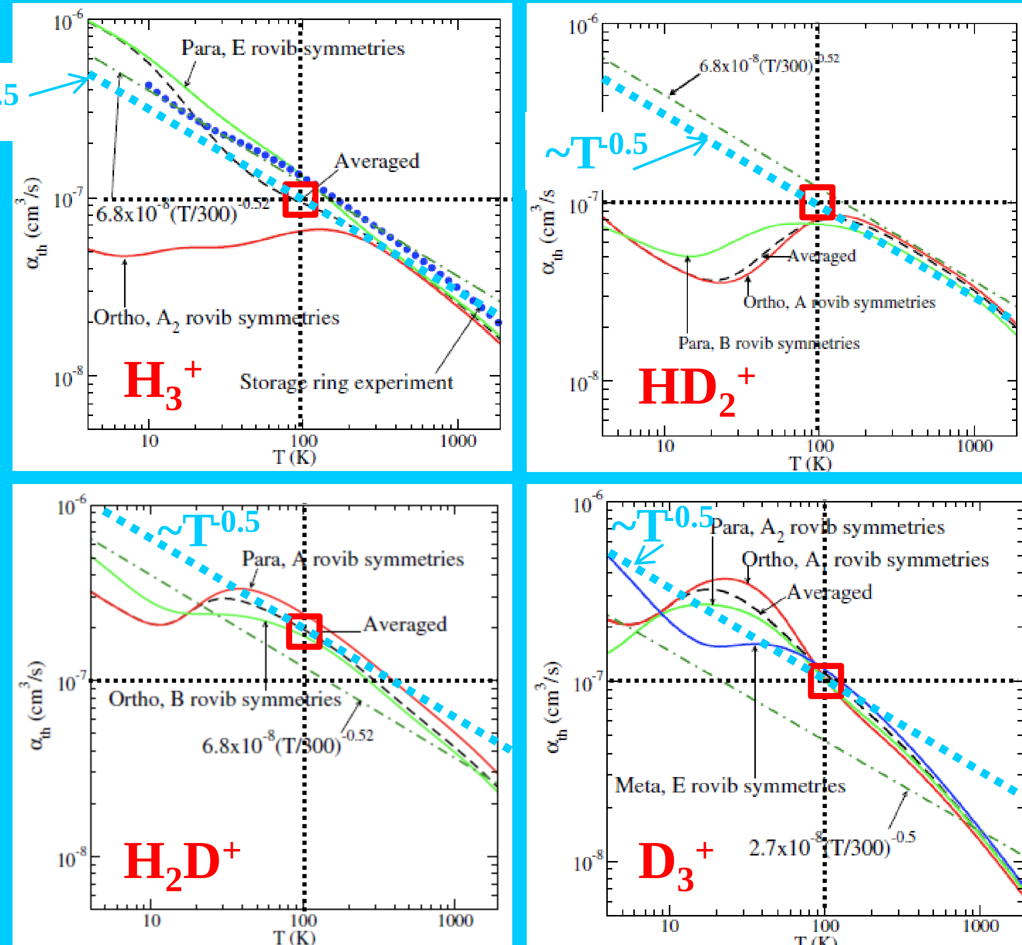

$\alpha \sim <v.\sigma>$

$\alpha \sim T^{-0.5}$

$$H_3^+ + e^- \xrightarrow{\alpha_{binH3}} \text{neutral products}$$

$$H_2D^+ + e^- \xrightarrow{\alpha_{binH2D}} \text{neutral products}$$

$$HD_2^+ + e^- \xrightarrow{\alpha_{binHD2}} \text{neutral products}$$

$$D_3^+ + e^- \xrightarrow{\alpha_{binD3}} \text{neutral products}$$

H_3^+

Nuclear spin dependence of H_3^+ recombination

B. J. McCall, et al. *Physical Review A* (2004)

H. Kreckel, J. Glosik, et al. Phys. Rev. Lett. 2005,

….2008, new improved calculations

Theory of Binary DR

The main mechanism (Jahn-Teller coupling) that leads to the fast dissociation when electron recombines with the ion requires <u>vibrational excitation of ionic core</u>

L. Pagani[1], C. Vastel[2], E. Hugo[3], V. Kokoouline[4], Chris H. Greene[5], A. Bacmann[6], E. Bayet[7], C. Ceccarelli[6], R. Peng[8], and S. Schlemmer[3]

M. Larsson, B.J. McCall, A.E. Orel (2008)

J. Glosik, R. Plasil, et al. *Phys. Rev. A*, 2009.

H. Kreckel, O. Novotny, et al., Phys. Rev. A（2010）.

K. N. Crabtree, N. Indriolo, et al., Astrophys. J. (2011)

J. Varju, M. Hejduk, J. Glosik, et al. *Phys. Rev. Lett.*, 2011.

P. Dohnal, M. Hejduk, J. Glosik, et al. *J. Chem. Phys.*, 2012.

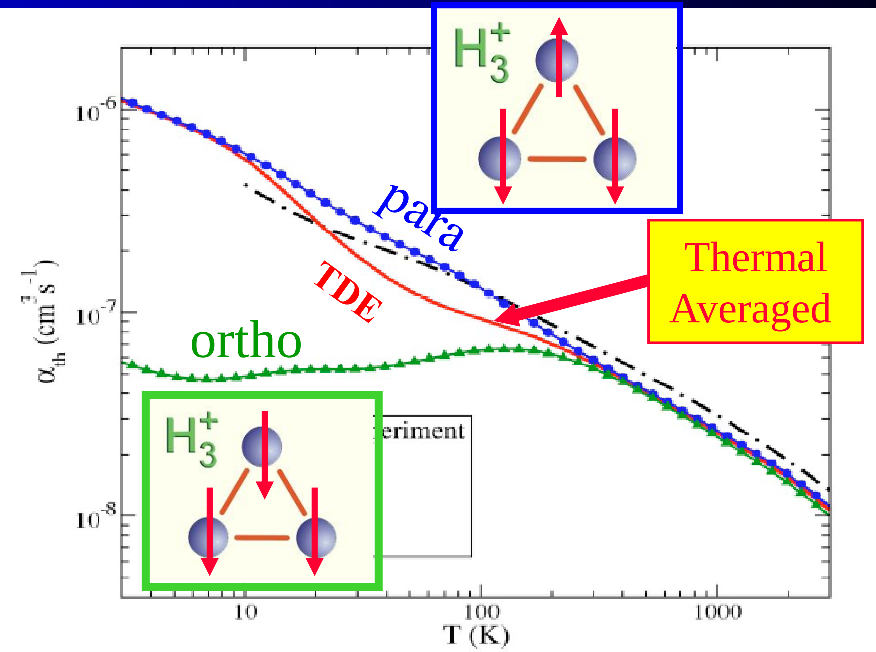

FIG. 5. (Color online) The present theoretical thermal rate coefficient for dissociative recombination of H_3^+ is compared with the experimental rate coefficient deduced from the storage ring experiment of McCall and co-workers (Refs. 9 and 10).

Doubts 2011

“Presently no rate coefficient measurement with a confirmed temperature below 300 K exists“.

Petrignani *et al.* Phys. Rev. A (2011)

Unfortunately the experiments on storage rings were stopped ☹ … ☹ …

3D 60 K

H_3^+ Potential curves

In the case of H_3^+, a simple 2-dimensional picture of molecular states suggests that recombination should be very inefficient

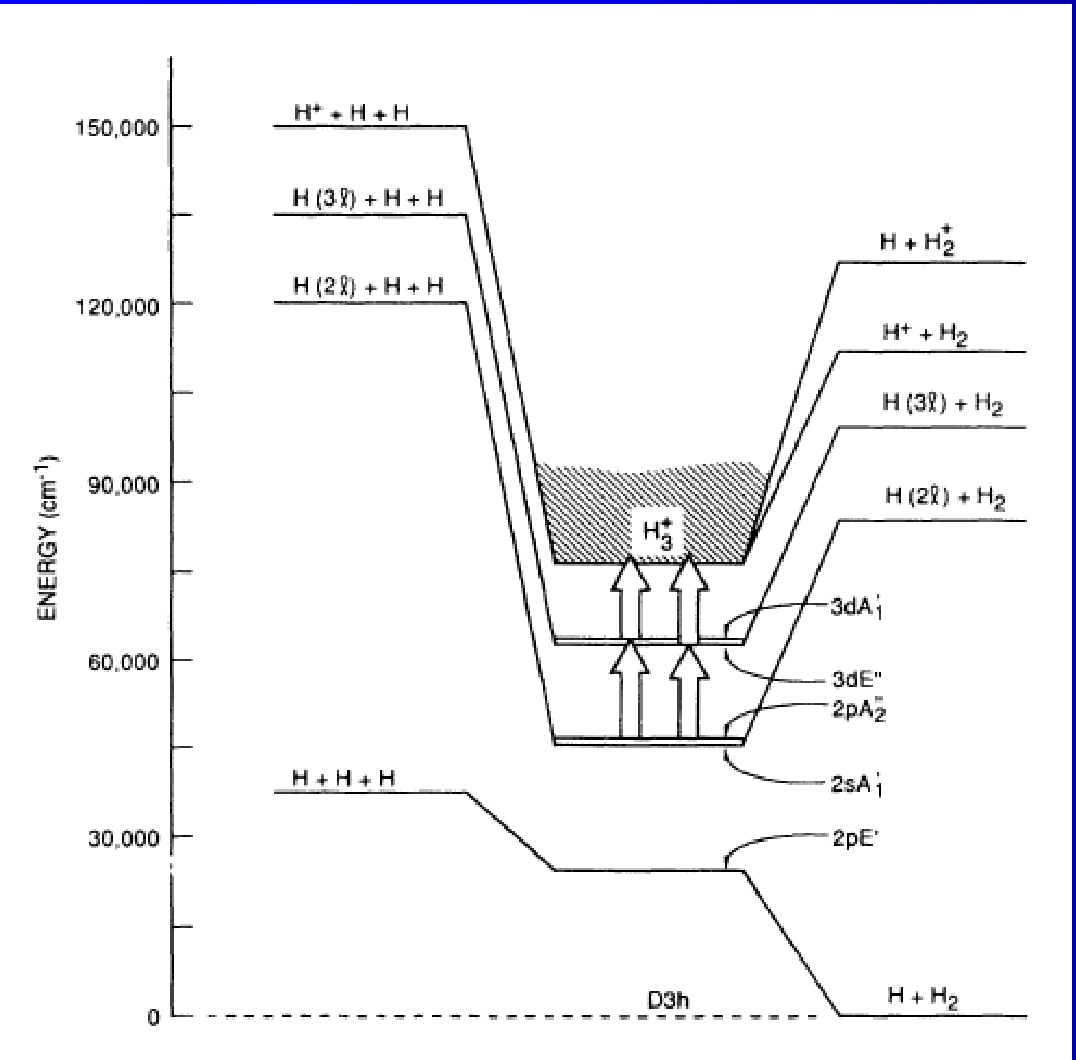

FIG. 1. Energy diagram of triatomic hydrogen (D_{3h} geometry) showing the location of the bound Rydberg states and the unstable ground state of H_3 in relation to the neutral and ionic dissociation limits.

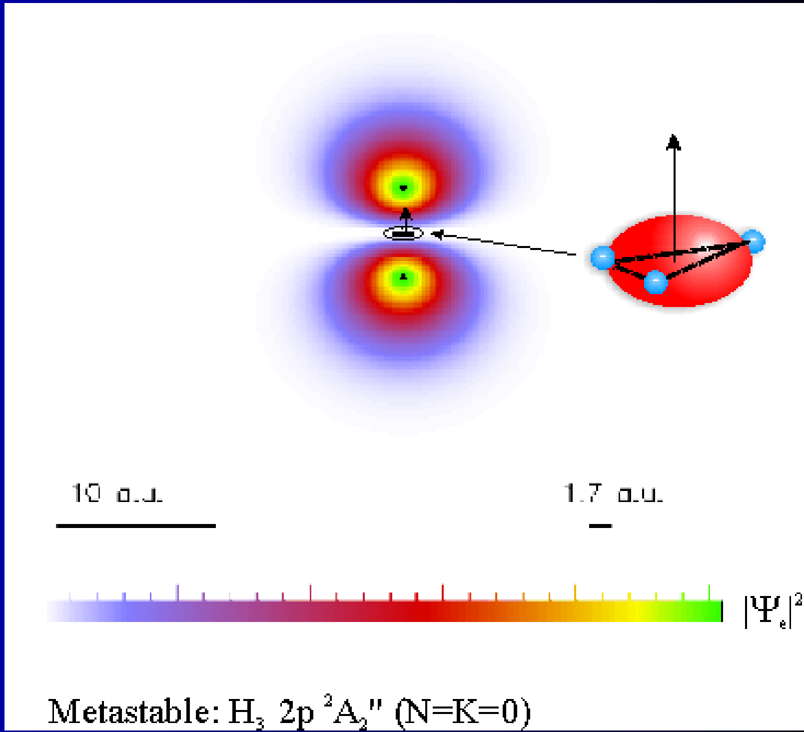

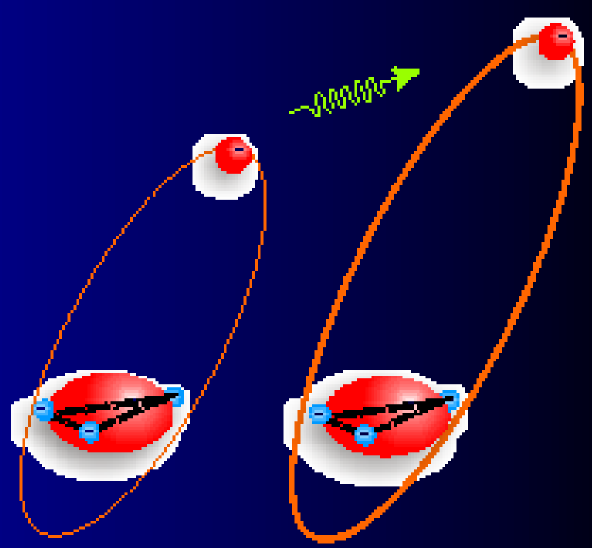

Line intensity H_3^+

High sensitivity required

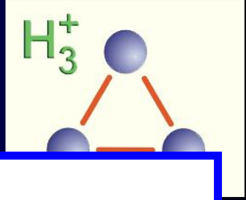

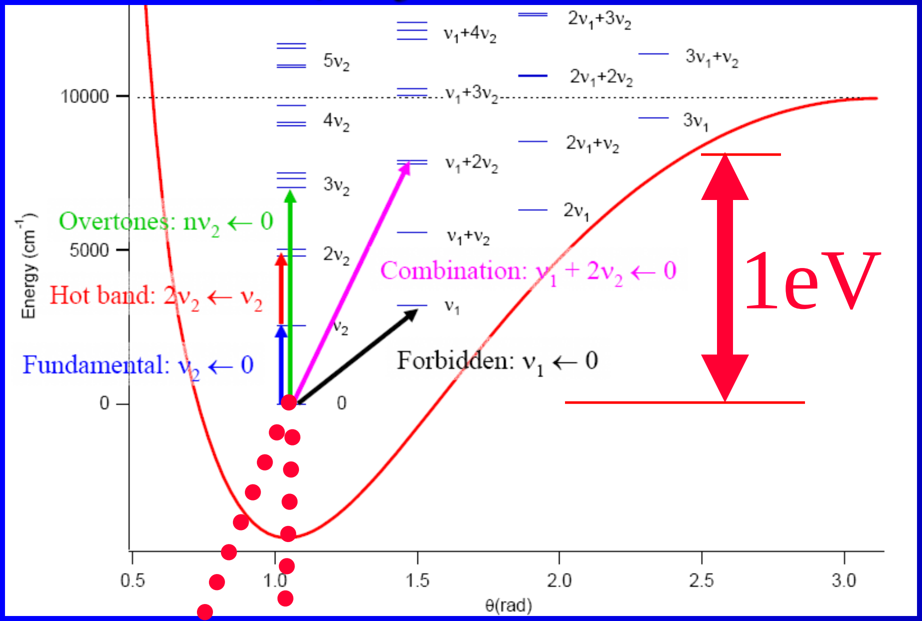

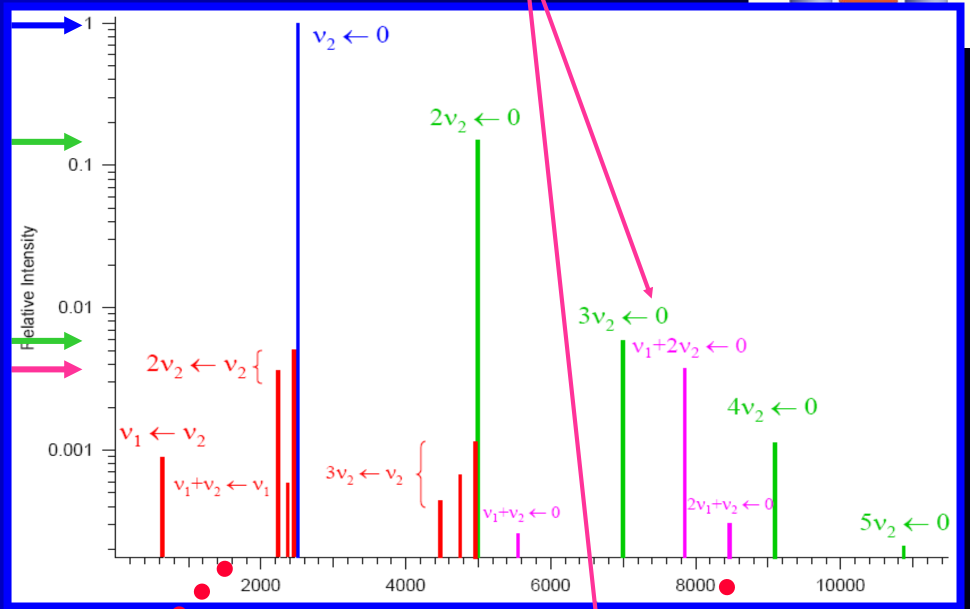

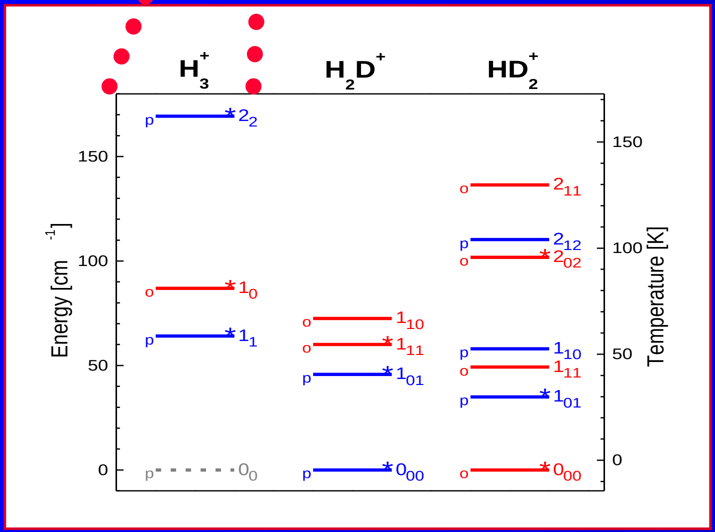

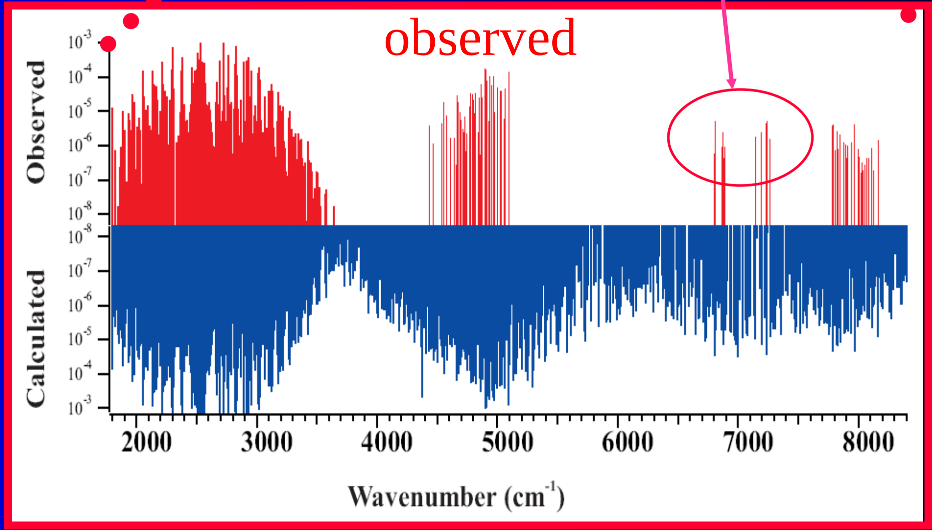

LIR - H_2D^+ and D_2H^+ precision of 10^{-8}

precision of $\Delta\nu/\nu = 10^{-8}$.

~26K

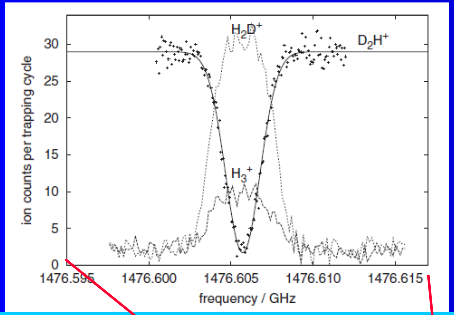

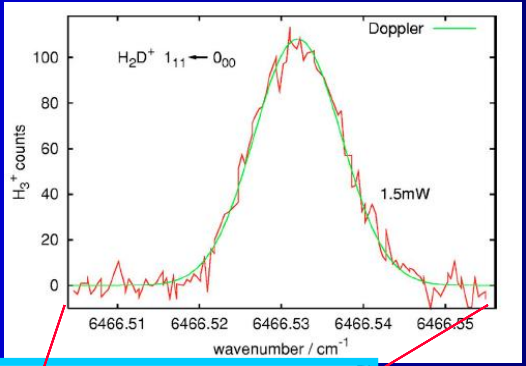

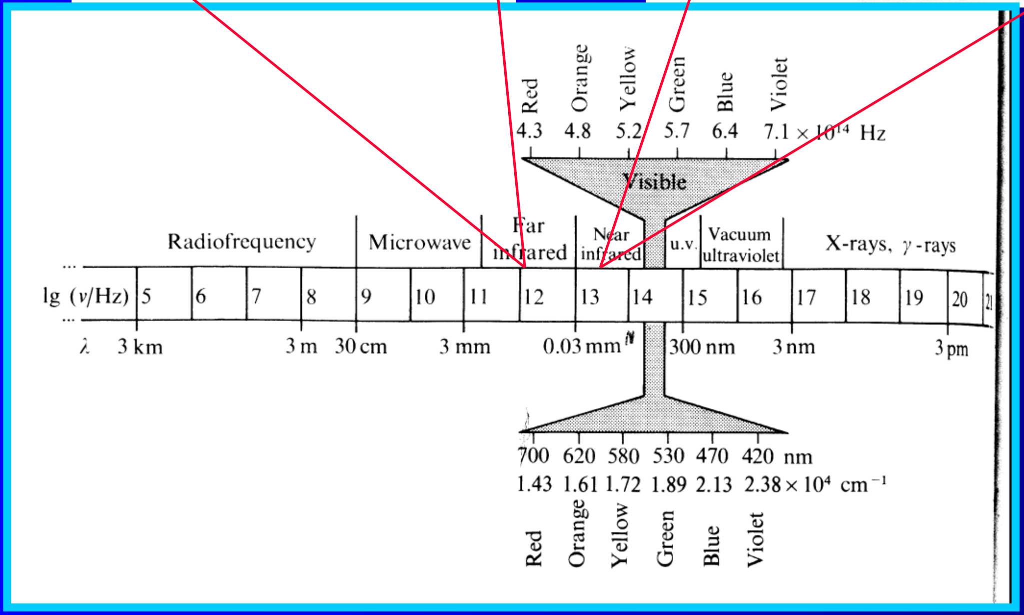

HD_2^+

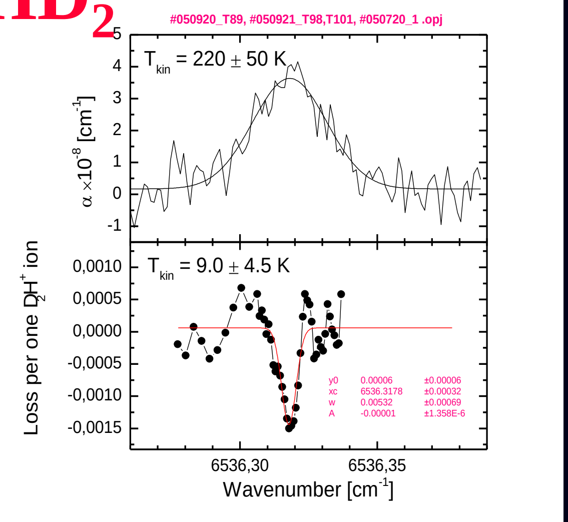

Stationary afterglow + Spectroscopic identification of recombining ions

$$\frac{d[H_3^+]}{dt} = -\alpha[H_3^+]n_e = -\alpha[H_3^+]^2$$

IR-CRDS

Laser absorption spectroscopy

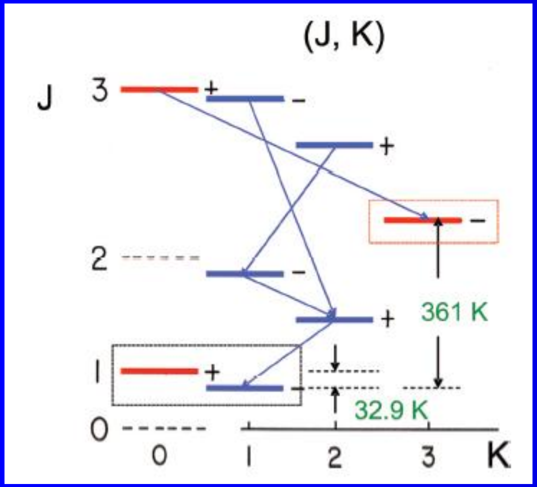

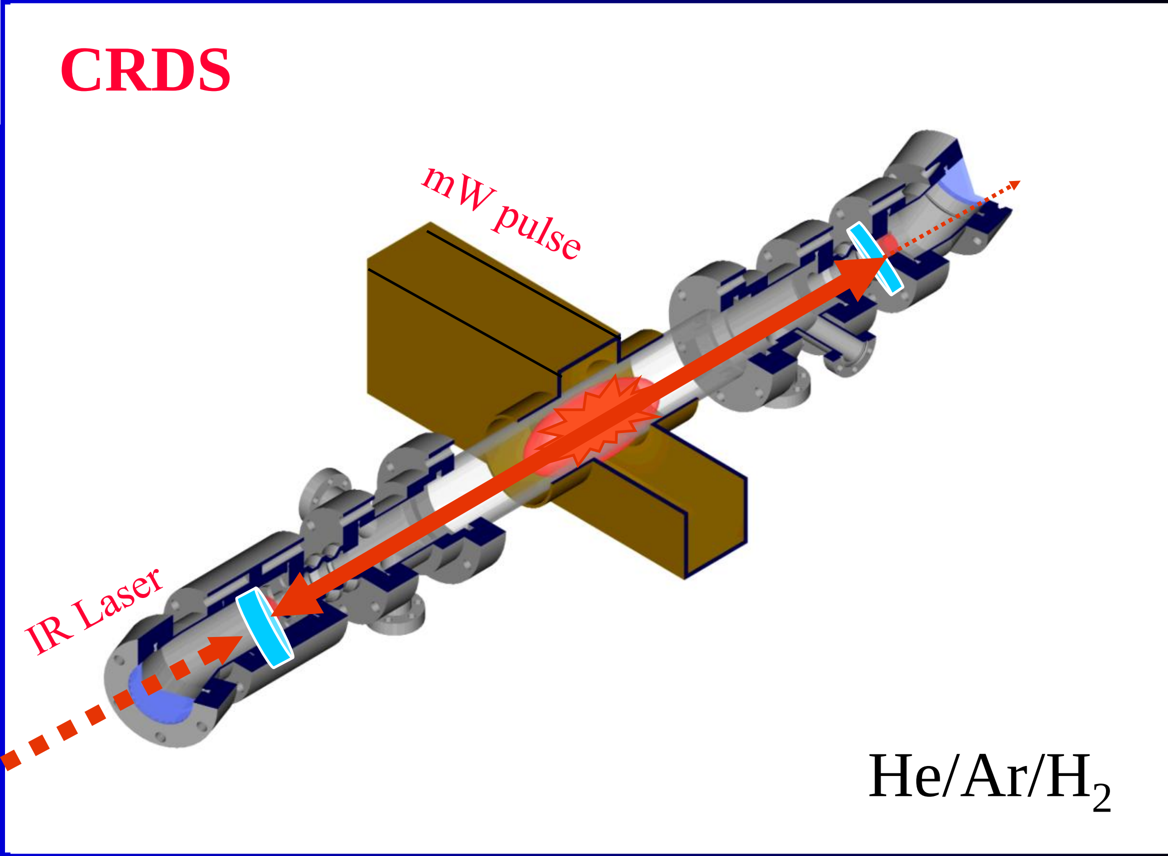

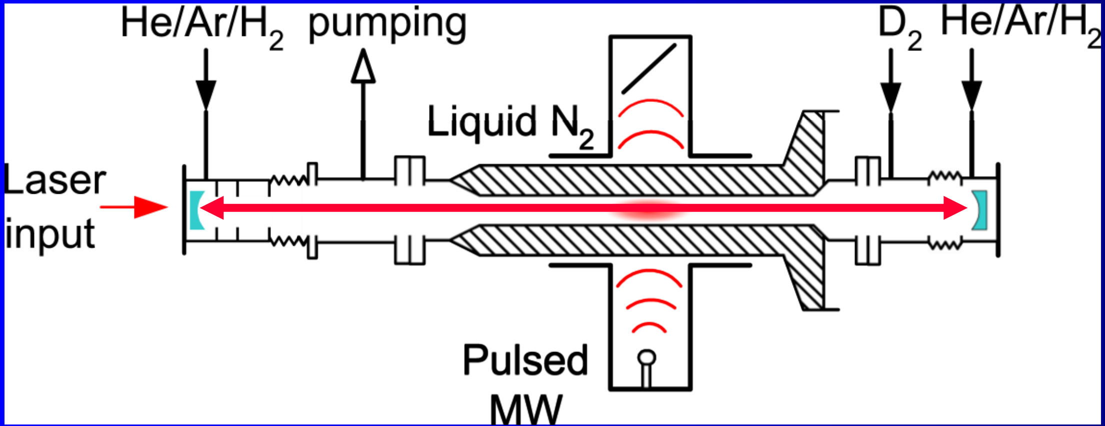

Spectrum - He/Ar/H_2 microwave discharge

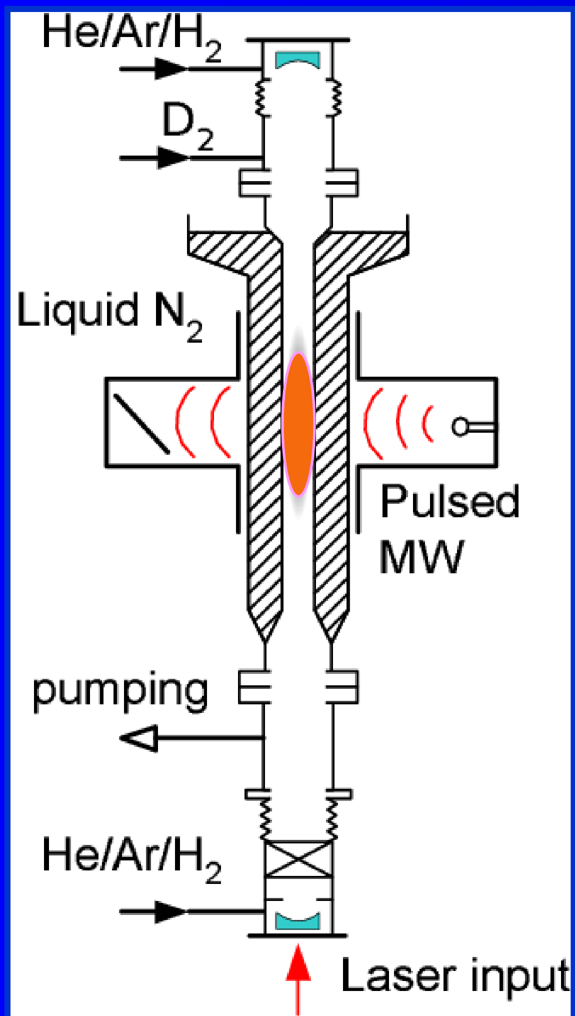

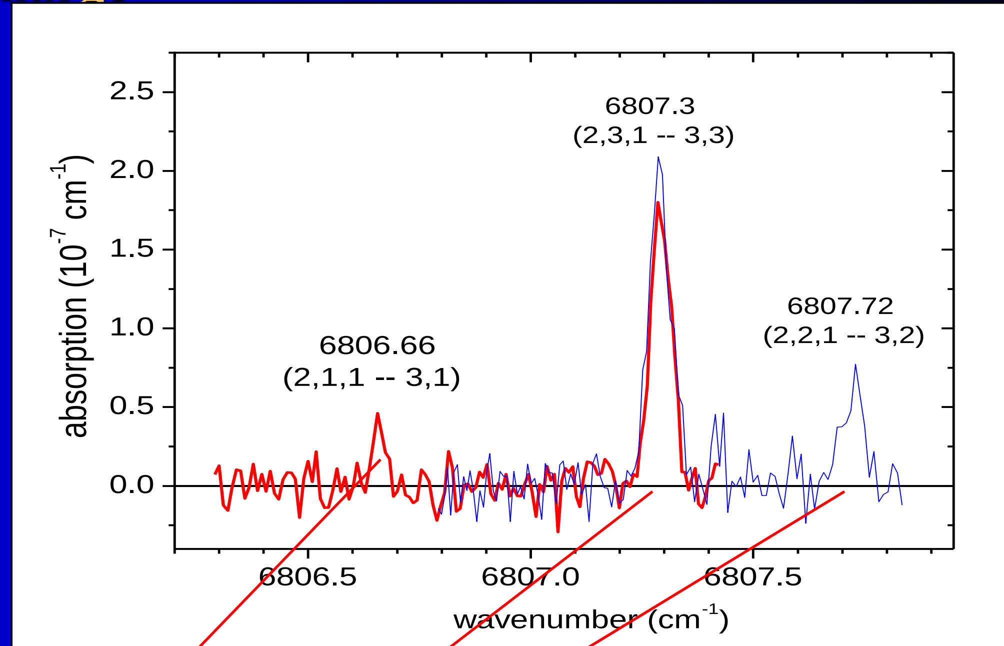

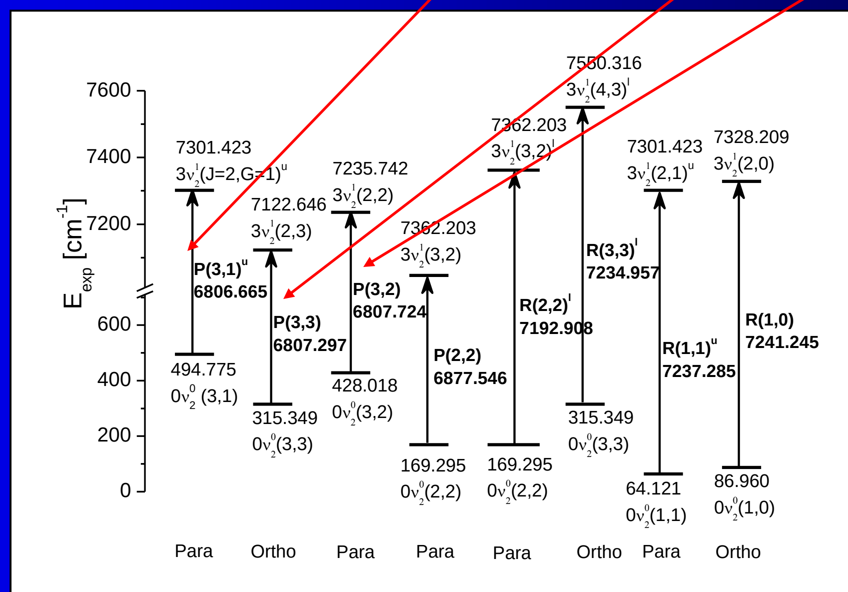

1469nm

1381nm

Pulsed discharge – plasma decay

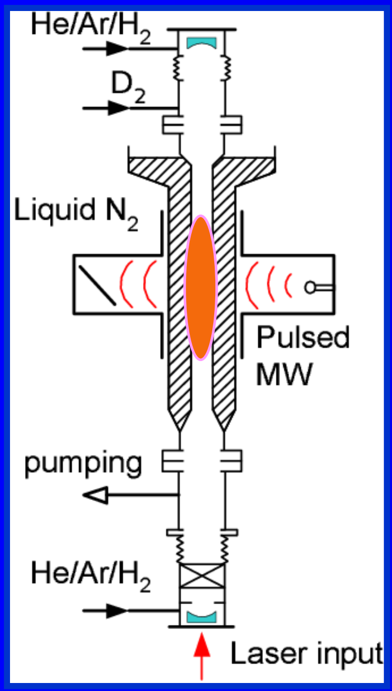

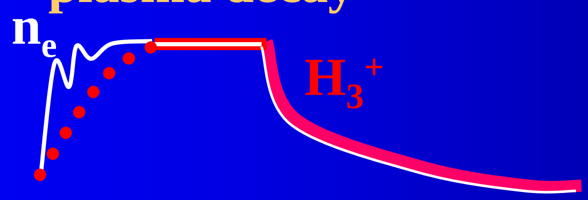

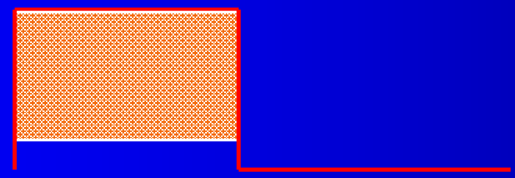

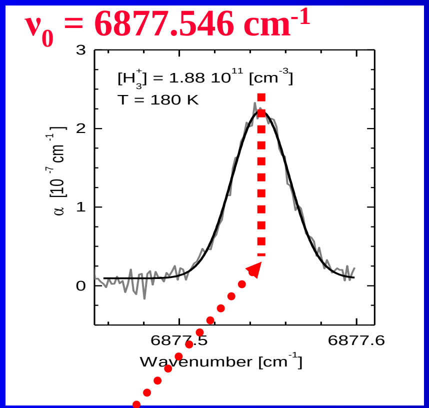

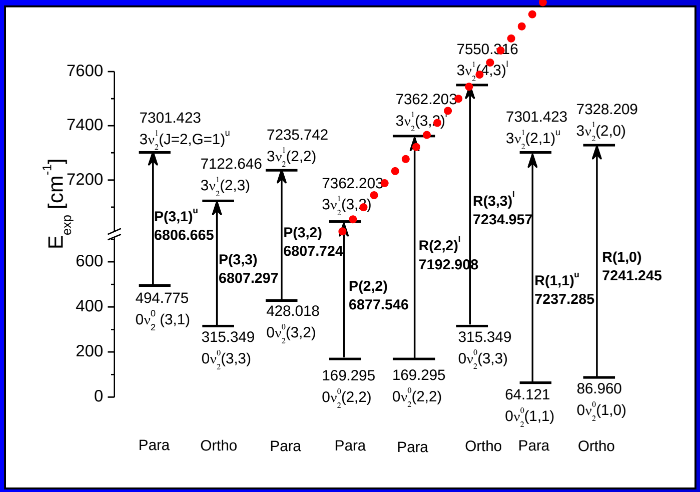

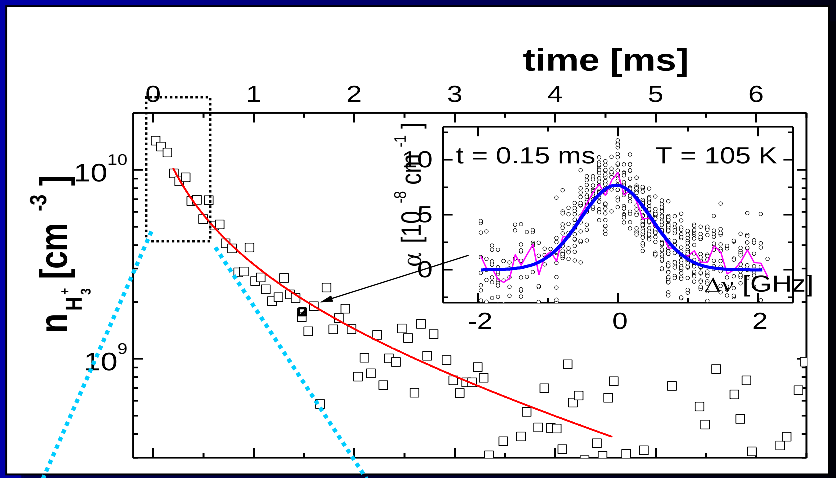

From Doppler broadening

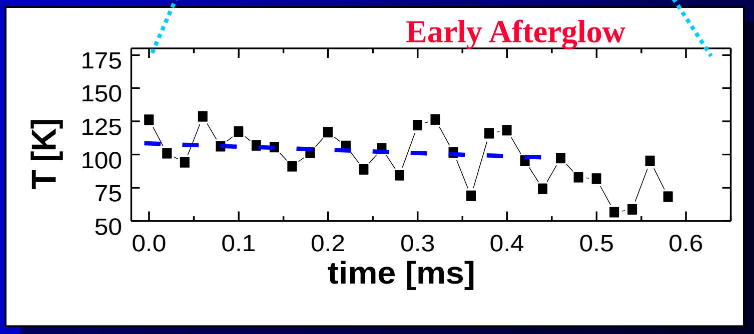

Absorption studies

He/Ar/H_2/D_2

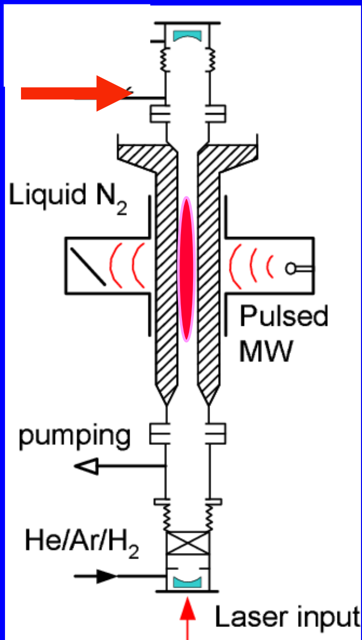

H_3^+

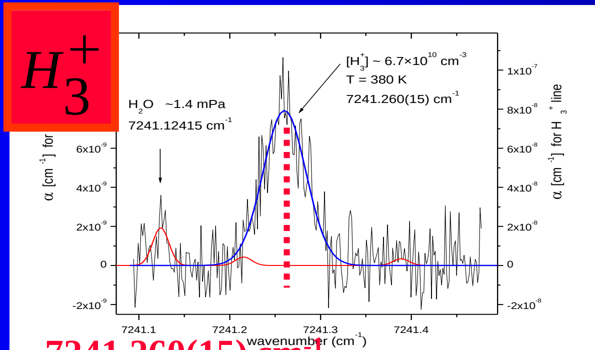

7241.260(15) cm^{-1}

H_2D^+ $(2\nu_2 + \nu_3 \leftarrow 0)$

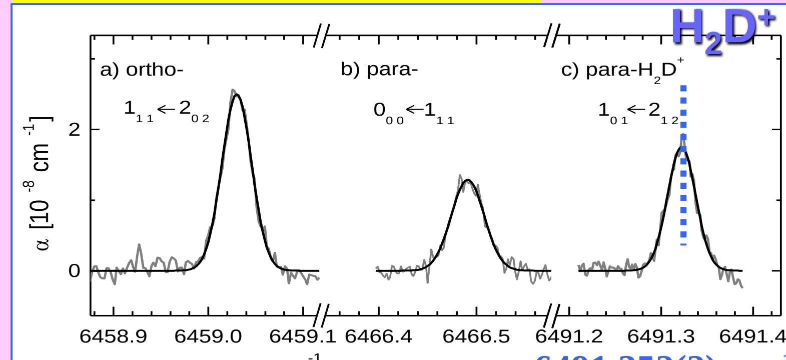

ν_0 = 6491.352(2) cm^{-1}

Combination band

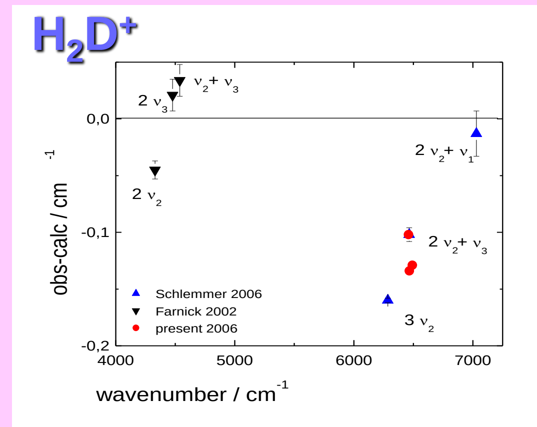

D_2H^+ $(\nu_1 + 2\nu_3 \leftarrow 0)$

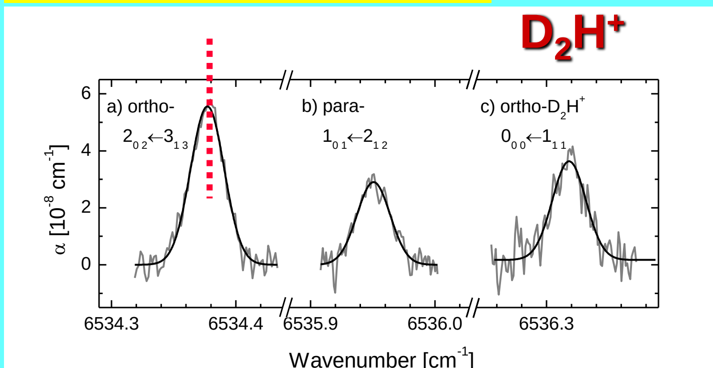

ν_0 = 6534.377(1) cm^{-1}

Combination band

E'[K]	Wavenumber [cm^{-1}] ν_{Exp}	ν_{Theor}	$\nu_{Theor} - \nu_{Exp}$
146.3	6534.377(1)	6534.374	0.003
50.2	6535.950(1)	6535.943	0.007
0	6536.319(2)	6536.301	0.018

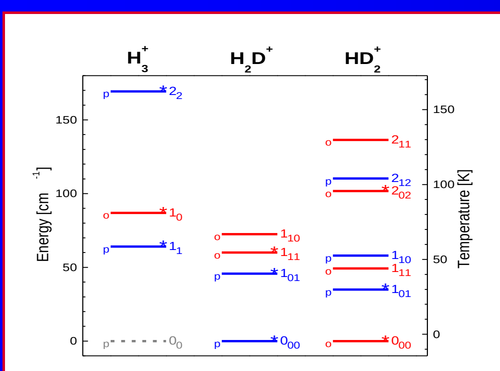

D_3^+ ???

Ionic composition of H_2/D_2 plasma

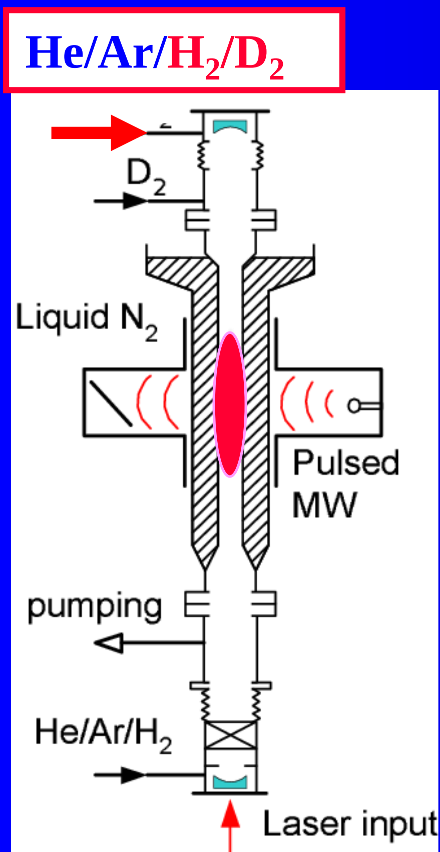

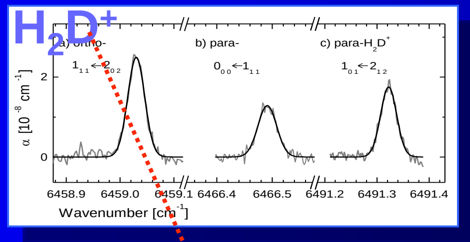

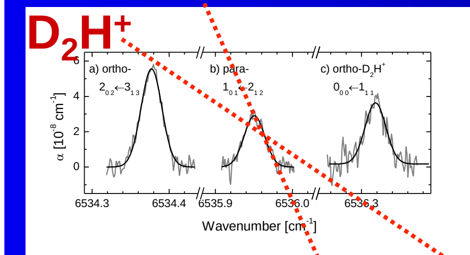

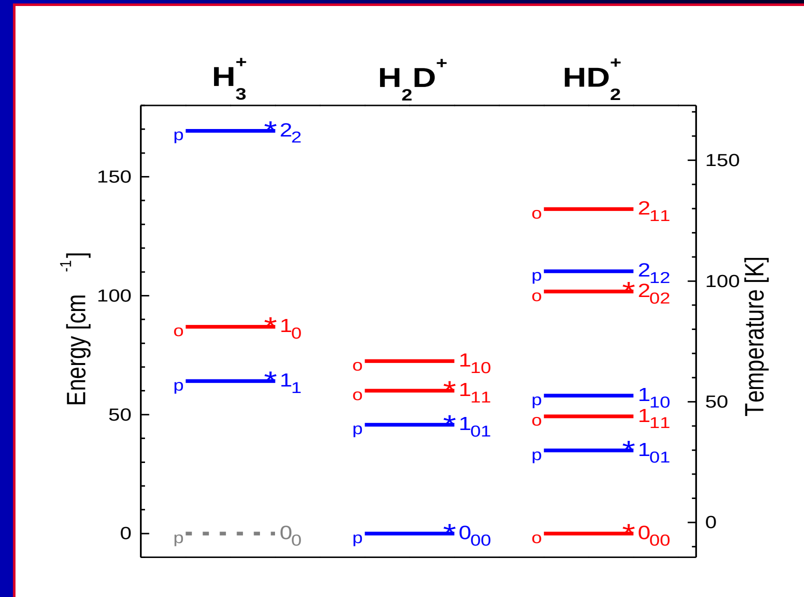

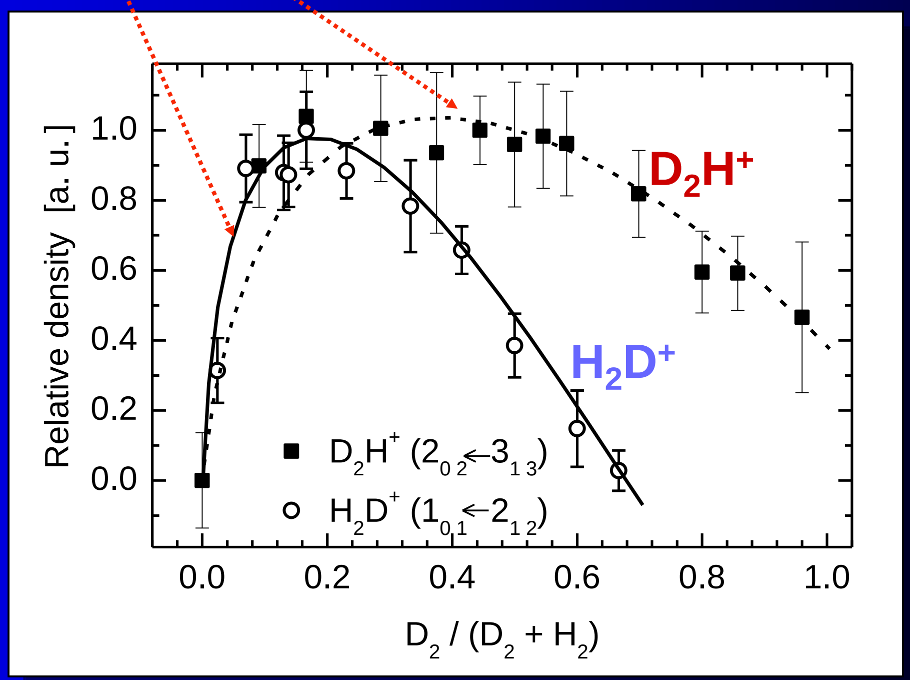

Observation of high population of deuterated molecules

The first detection of deuterated molecules were made in the early 1970s……. Observed enhancement of D in molecules

H_2D^+	Stark	(1999)	1_{10}–1_{11} transition of ortho- emission from young stellar object NGC 1333 IRAS4A.
H_2D^+	Caselli	(2003)	detected towards L1544.
HD_2^+	Vastel	(2004)	the first detection
CH_2DOH…	Parise	(2003, 2004)	have detected 4 isotopomers of deuterated methanol
NHD_2/NH_3	Roueff	(2000)	
	Loinard	(2001)	is 0.005 in the cold cloud L134N and 0.03 in the low-mass protostar 16293 E
D_2CO/H_2CO	Loinard	(2002)	
	Bacmann	(2003)	is between 0.01 and 0.4 in a low-mass protostars and prestellar cores
NH_2D/NH_3	J. Hatchell	(2003)	high ratios~4–33% in protostellar cores
ND_3/NH_3	Lis	(2002)	ratio ~10^{-3} cold dense Barnard 1cloud
	Tak	(2002)	Class 0 protostar NGC 1333 IRAS4A

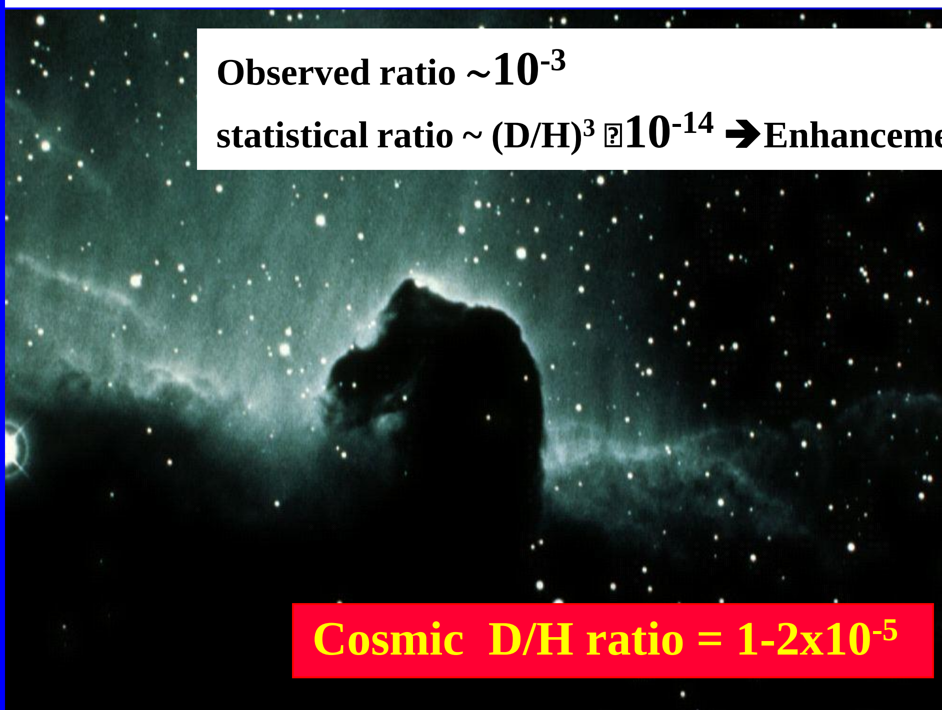

Observed ratio ~10^{-3}

statistical ratio ~ $(D/H)^3$ ≈ 10^{-14} ➔ Enhancement of 10^{11}

Cosmic D/H ratio = 1-2x10^{-5}

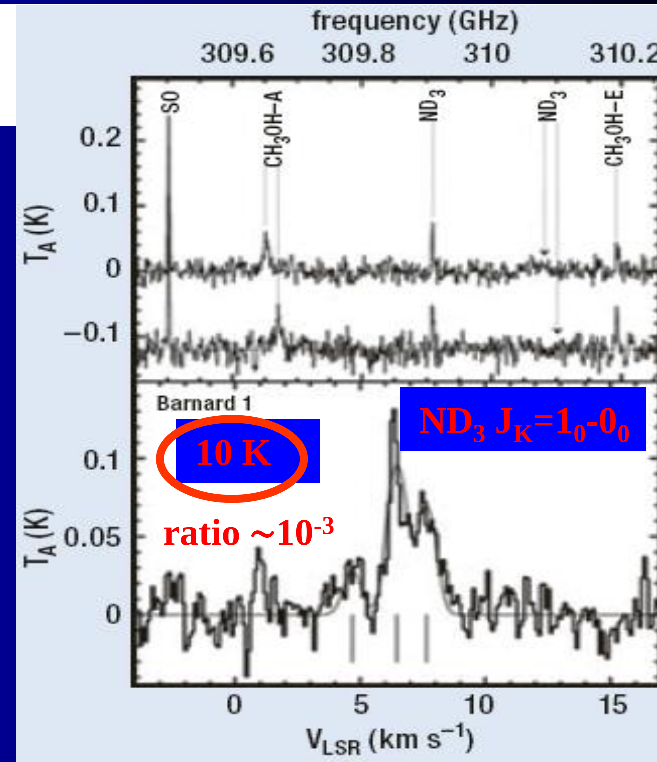

2: Spectrum of ND_3 towards the dark cloud B1.
(Lis *et al.* 2002 *ApJ* 571 L55)

High population of deuterated molecules

Cosmic D/H ≈ 10^{-5}

XD/XH ≈ 10^{-1}-10^{-3}

XD_2 / XH_2 ≈ 10^{-2}

XD_3 / XH_3 ≈ 10^{-3}

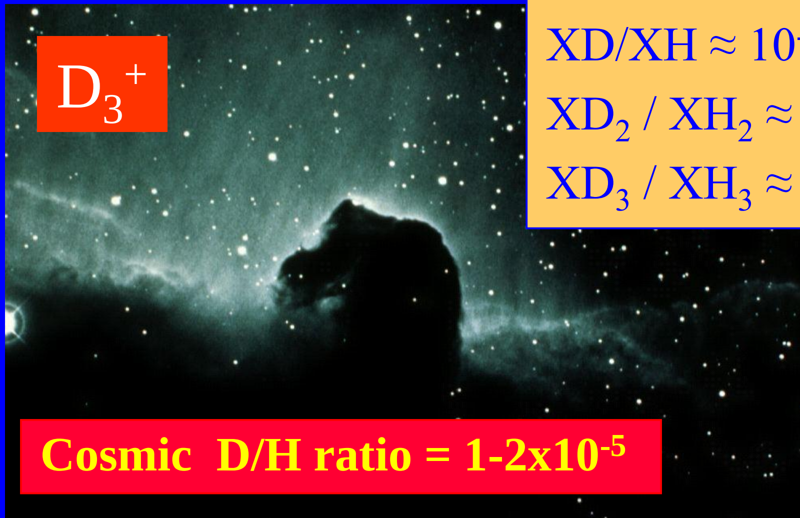

Species	Observed ratio
NH_2D/NH_3	0.01
$HDCO/H_2CO$	0.005-0.11
DCN/HCN	0.023
DNC/HNC	0.015
C_2D/C_2H	0.01
DCO^+/HCO^+	0.02
N_2D^+/N_2H^+	0.08
DC_3N/HC_3N	0.03-0.1
$HDCS/H_2CS$	0.02

H_3^+ D_3^+

HD	H_2D^+	D_2H^+
N_2D^+	DCO^+	DCN
DNC	HDCS	D_2CS
HDO	DC_3N	DC_5N
C_3HD	HDCO	D_2CO
CH_3OD	CH_2DOH	CHD_2OH
CD_3OH	CH_2DCN	NH_2D
NHD_2	ND_3	CHD_2CCH
CH_3CCD	C_2D	C_4D
HDS	D_2S	

Deuterated molecules that have been detected in interstellar clouds as of February 2005.

<u>Gas phase reactions,</u>

<u>ion-molecule reactions,</u>

<u>recombination</u>

Grain surface reactions

Physics of condensation and evaporation from grain surface

Different views
& different plasmas

H_3^+ and its interaction of with e^- is **FUNDAMENTAL**

If you understand hydrogen,
you understand all
that can be understood.
(*V. Weisskopf & G. Herzberg*).

$H_3^+ + e^-$

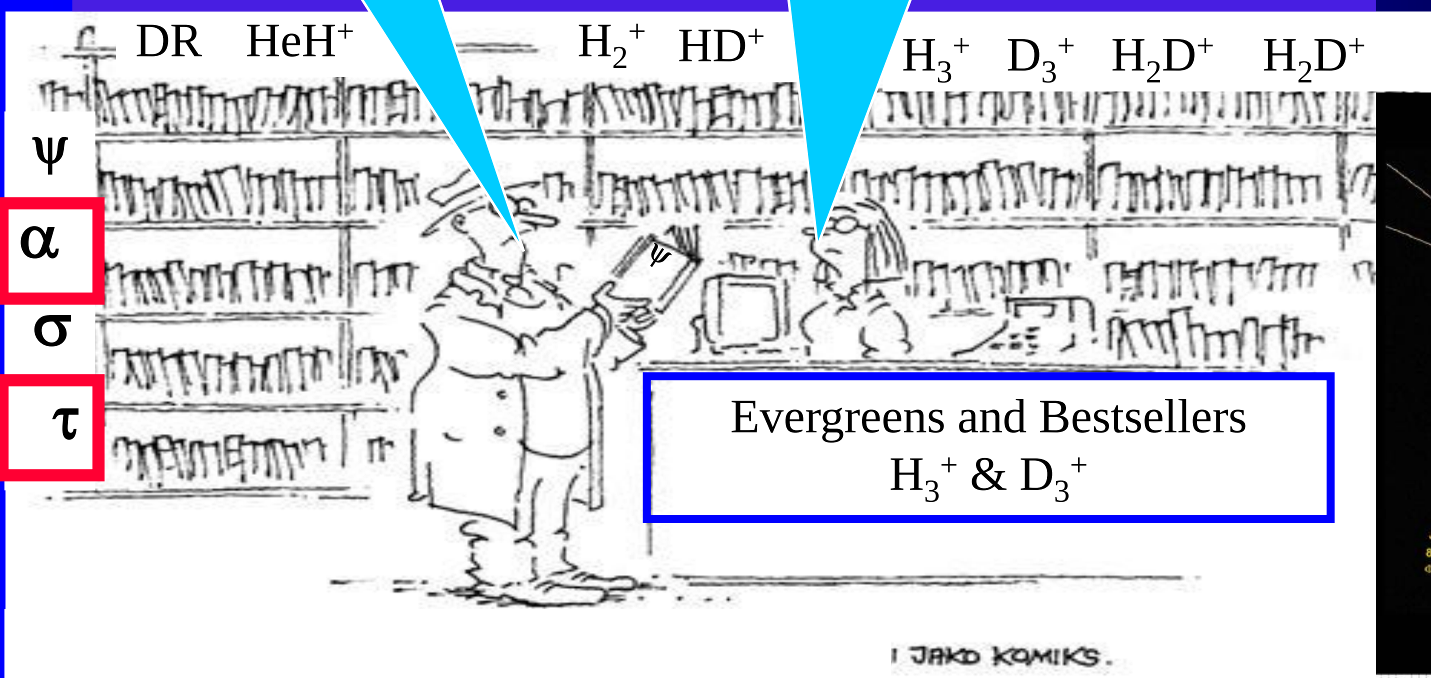

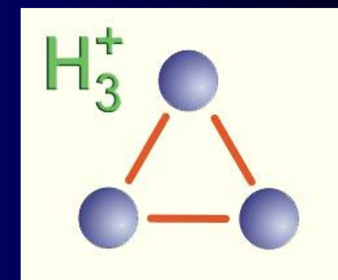

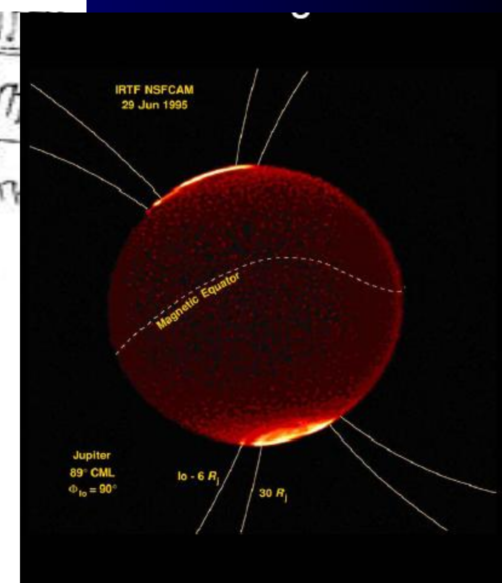

J.E.P. Connerney and T. Satoh,
Phil. Trans. R. Soc. Lond. A358, 2471 (2000)

H_3^+ , H_2D^+, HD_2^+ D_3^+ are fundamental

PRL 102, 023201 (2009) PHYSICAL REVIEW LETTERS

Jahn-Teller Interactions in the Dissociative Recombination of H_3^+

Ch. Jungen[1,*] and S. T. Pratt[2]

A&A 494, 623–636 (2009)
DOI: 10.1051/0004-6361:200810587
© ESO 2009
Astronomy & Astrophysics

Chemical modeling of L183 (L134N): an estimate of the ortho/para H_2 ratio*

L. Pagani[1], C. Vastel[2], E. Hugo[3], V. Kokoouline[4], C. H. Greene[5], A. Bacmann[6], E. Bayet[7], C. Ceccarelli[6], R. Peng[8], and S. Schlemmer[3]

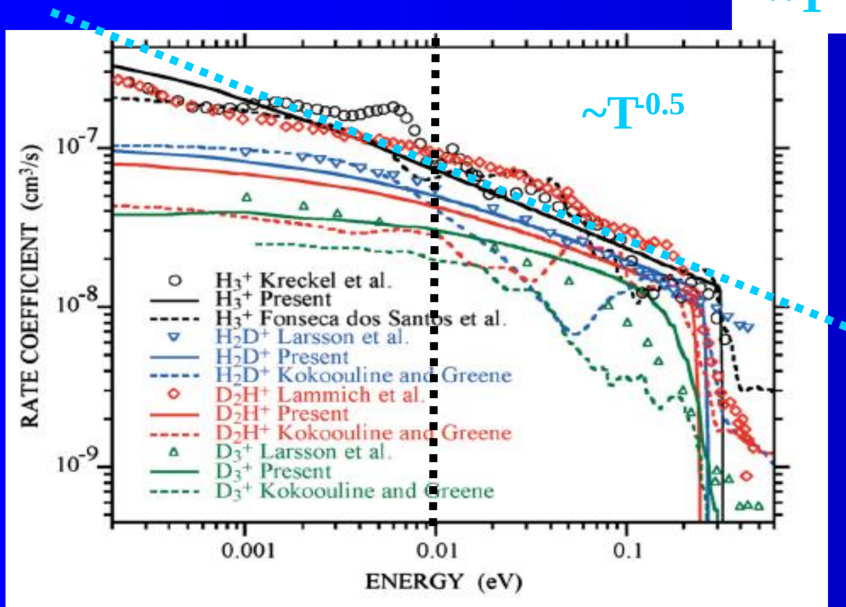

FIG. 3 (color). The DR rate coefficient of an electron and H_3^+, H_2D^+, D_2H^+, and D_3^+ as a function of collision energy. H_3^+

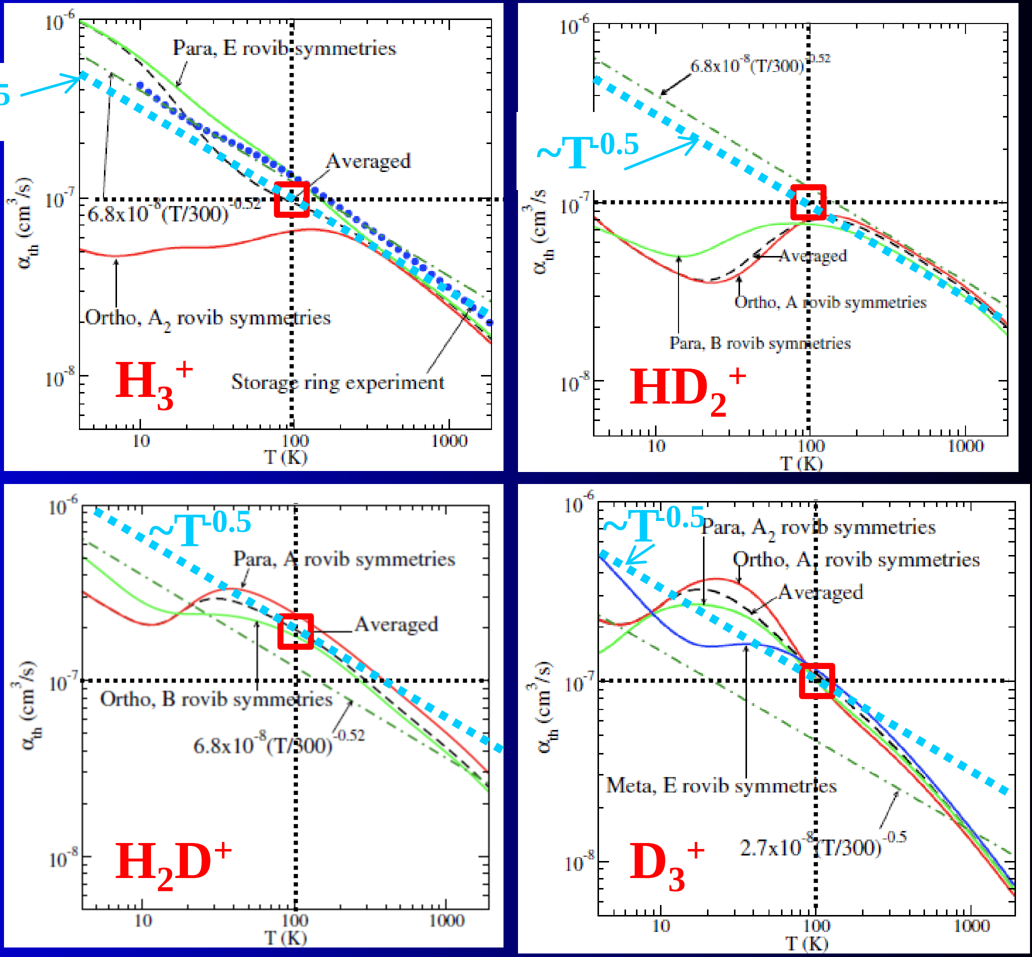

$$\alpha \sim \langle v.\sigma \rangle$$

$$\alpha \sim T^{-0.5}$$

$$H_3^+ + e^- \xrightarrow{\alpha_{binH3}} \text{neutral products}$$

$$H_2D^+ + e^- \xrightarrow{\alpha_{binH2D}} \text{neutral products}$$

$$HD_2^+ + e^- \xrightarrow{\alpha_{binHD2}} \text{neutral products}$$

$$D_3^+ + e^- \xrightarrow{\alpha_{binD3}} \text{neutral products}$$

H_3^+ interaction with e^-

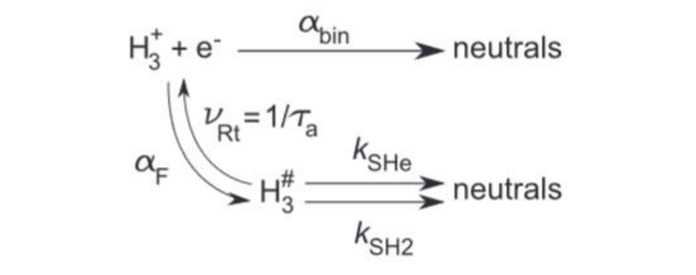

FIG. 1. The scheme of the proposed H_3^+ recombination mechanism. Used symbols are explained in the text.

Plasma Sources Sci. Technol. **24** (2015) 065017

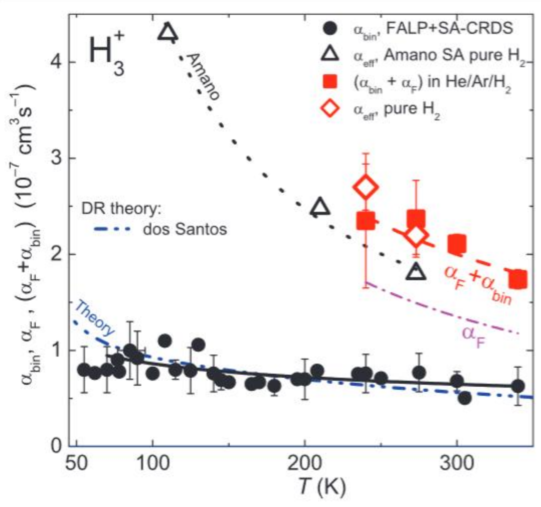

Figure 5. Temperature dependences of α_{bin}, α_F, and their sum ($\alpha_{bin} + \alpha_F$). The diamonds and squares indicate ($\alpha_{bin} + \alpha_F$) measured in pure H_2 and in He/Ar/H_2 mixture, respectively. The fit of the data (dashed line) gives the temperature dependence: $(\alpha_{bin} + \alpha_F) = (2.0 \pm 0.4) \times 10^{-7}(T/300\ \mathrm{K})^{-(0.81\pm0.30)}$ cm^3 s^{-1}. The filled circles indicate the values of α_{bin} for H_3^+ ions in He/Ar/H_2 mixtures that were obtained in several stationary and flowing afterglow experiments (for details see [22, 26]). The full line indicates the dependence $\alpha_{bin} = (6.5 \pm 1.4) \times 10^{-8}(T/300\ \mathrm{K})^{-(0.26\pm0.07)}$ cm^3 s^{-1} obtained by fitting α_{bin} data at temperatures 80–340 K. Included are the present data and data from [22, 26]. The dependence of α_F on temperature (dot–dashed line) was obtained by subtracting α_{bin} (full line) from the sum of ($\alpha_{bin} + \alpha_F$) (dashed line). The rate coefficients measured by Amano [30] in pure H_2, assumed to be due to binary recombination only, are plotted as open triangles for comparison. The dotted line indicates a fit to Amano's data: $\alpha_{Amano} = 1.7 \times 10^{-7}(T/300\ \mathrm{K})^{-0.94}$ cm^{3}s^{-1}. The theoretical temperature dependence of the binary rate coefficient of dissociative recombination of H_3^+ ions calculated by Fonseca dos Santos *et al* [12] is plotted by a double dot–dashed line denoted Theory.

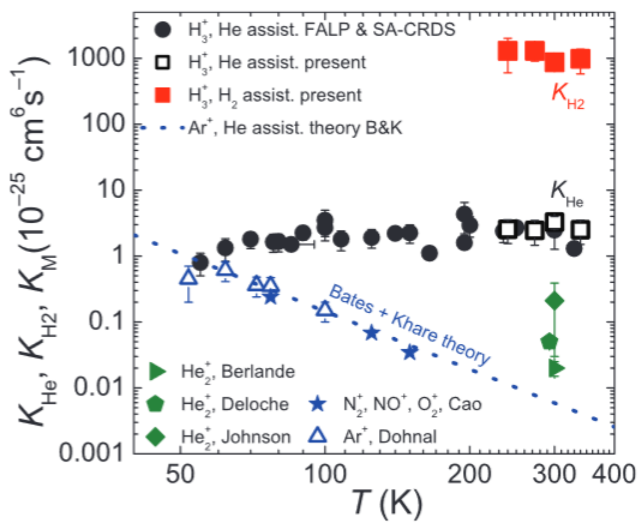

Figure 6. Temperature dependences of the three-body rate coefficients K_{H2} (closed squares) and K_{He} (open squares) of H_2 and He assisted recombination of H_3^+ ions. Closed circles: K_{He} of H_3^+ ions obtained in our previous experiments [21, 23, 24, 34]. Open triangles: Three-body recombination rate coefficients of He-assisted collisional radiative recombination K_{HeAr+} of Ar^+ ions measured in a Cryo-FALP II experiment [50]. Filled stars: K_{He-CRR} as measured by Cao *et al* [51] for a mixture of atmospheric ions in He. Dotted line: Theoretical dependence of Bates and Khare [32] scaled for Ar^+ ions in He by the reduced mass. Full triangle, pentagon and diamond indicate three-body rate coefficients measured for He_2^+ ions in helium by Berlande [52], Deloche [53] and Johnson [54], respectively.

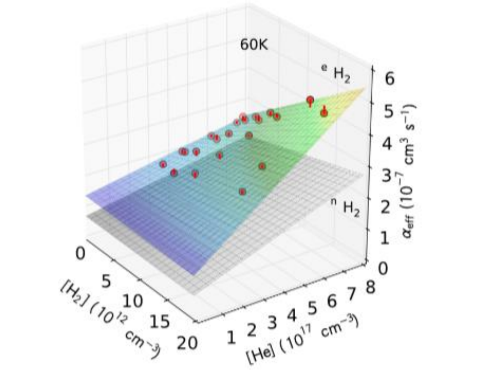

FIG. 7. Cryo-FALP II data. Dependence of $^e\alpha_{eff}$ and $^n\alpha_{eff}$ on [He] and [H_2] measured at $T = 60$ K in experiments with $^eH_2$ and with $^nH_2$, respectively. The upper surface is a fit of Eq. (6) to the data (indicated by circles) obtained with $^eH_2$. The lower surface represents a fit of Eq. (6) to the data obtained with $^nH_2$ (data points are omitted for clarity). The data points deviate from the surfaces by amounts on the order $<2\times10^{-8}$ cm^3 s^{-1} as is shown by red lines connecting the data points with the plane. The parameters of the fits are listed in Table I.

H_3^+ interaction with e^-

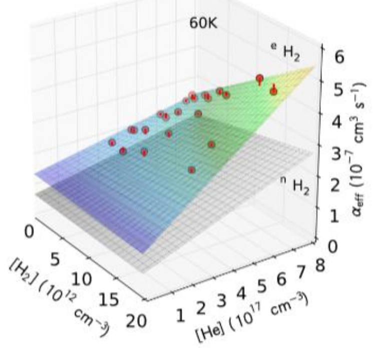

FIG. 7. Cryo-FALP II data. Dependence of $^e\alpha_{eff}$ and $^n\alpha_{eff}$ on [He] and [H_2] measured at $T = 60$ K in experiments with $^eH_2$ and with $^nH_2$, respectively. The upper surface is a fit of Eq. (6) to the data (indicated by circles) obtained with $^eH_2$. The lower surface represents a fit of Eq. (6) to the data obtained with $^nH_2$ (data points are omitted for clarity). The data points deviate from the surfaces by amounts on the order $<2\times10^{-8}$ cm^3 s^{-1} as is shown by red lines connecting the data points with the plane. The parameters of the fits are listed in Table I.

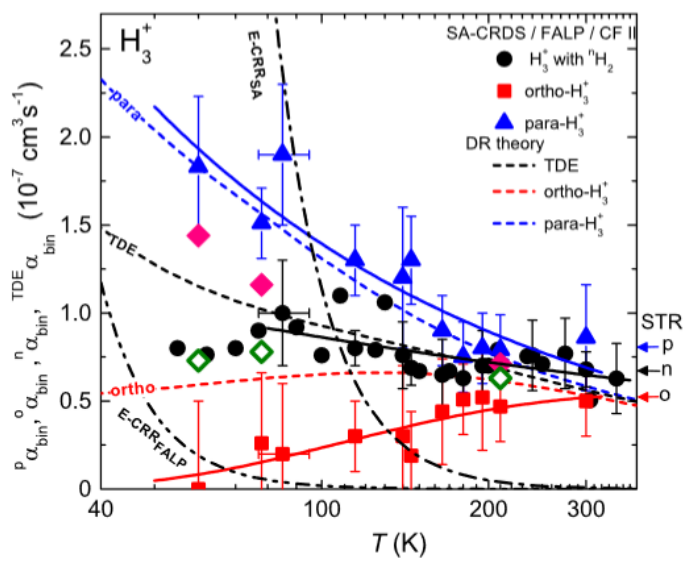

FIG. 8. Cryo-FALP II and SA-CRDS. Nuclear spin state-specific binary recombination rate coefficients measured in Cryo-FALP II, FALP, and SA-CRDS experiments. Triangles and squares indicate $^p\alpha_{bin}$ and $^o\alpha_{bin}$, respectively. The values at 85 K, 140 K, 165 K, and 195 K were taken from our previous experiments.[19] The values of $^n\alpha_{bin}$ (circles) were measured in the Cryo-FALP II, FALP, and SA-CRDS experiments and some data were taken from our previous studies.[19,41] The diamonds refer to $^n\alpha_{bin}$ (open diamonds) and $^e\alpha_{bin}$ (closed diamonds) measured in the present Cryo-FALP II experiment. The full lines are fits to $^p\alpha_{bin}$, $^o\alpha_{bin}$, and $^n\alpha_{bin}$ to the function in Eq. (7) that is used in astrophysical databases. For details and for the parameters of the fits see the text and Table II. The arrows on the right hand side of the figure denoted as p, o, and n indicate the values of $^p\alpha_{bin}$, $^o\alpha_{bin}$, and $^n\alpha_{bin}$ obtained in CRYRING,[13] respectively. The dashed lines indicated as para, ortho, and thermodynamic equilibrium (TDE) are theoretical dependences for para–H_3^+, ortho–H_3^+, and for H_3^+ ions in TDE.[33,35] The dashed-dotted lines E–CRR$_{SA}$ and E–CRR$_{FALP}$ are effective binary rate coefficients of ternary E–CRR calculated for electron number densities n_e(SA-CRDS) $= 3\times10^{10}$ cm^{-3} and n_e(Cryo-FALP II) $= 5\times10^8$ cm^{-3}.[19,27–29]

H_3^+ interaction with e^-

THE JOURNAL OF CHEMICAL PHYSICS **136**, 244304 (2012)

Binary and ternary recombination of para-H_3^+ and ortho-H_3^+ with electrons: State selective study at 77–200 K

Petr Dohnal,[1] Michal Hejduk,[1] Jozef Varju,[1] Peter Rubovič,[1] Štěpán Roučka,[1] Tomáš Kotrík,[1] Radek Plašil,[1] Juraj Glosík,[1] and Rainer Johnsen[2]

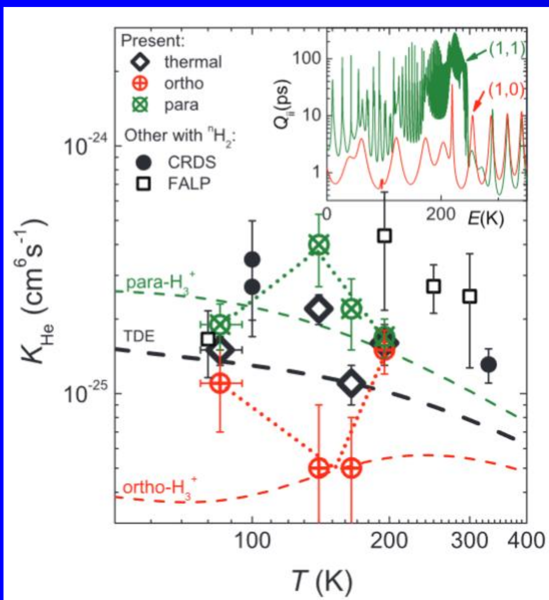

FIG. 12. Ternary recombination rate coefficients $^{p}K_{He}$, $^{o}K_{He}$, and $^{n}K_{He}$. The data obtained in previous CRDS (closed circles) and FALP/SA (open squares) experiments[33,34] are also shown. The dotted lines drawn through the para and ortho data are only meant to guide the eye. In the insert diagonal elements Q_{ii} of lifetime Matrix **Q** for the two lowest initial rotational states of H_3^+ are plotted. Each curve is labeled with the corresponding quantum numbers (J,G).[8,34]

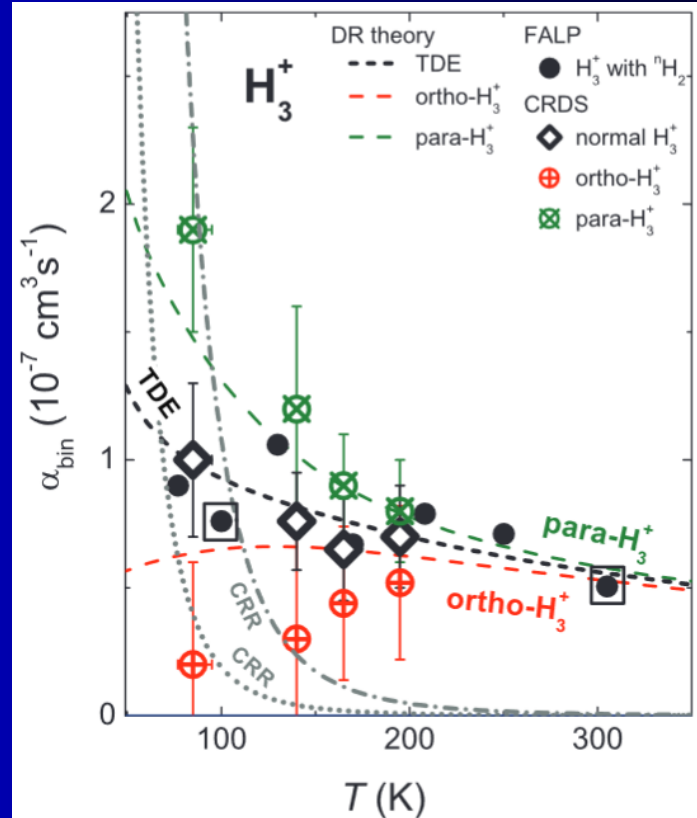

FIG. 13. Measured temperature dependences of the binary recombination rate coefficients $^{n}\alpha_{bin}$, $^{p}\alpha_{bin}$, and $^{o}\alpha_{bin}$ for normal-H_3^+ (measured in experiments with $^{n}H_2$), para-H_3^+, and ortho-H_3^+, respectively (see also Ref. 78). Previous FALP data[8,33,34] measured with $^{n}H_2$ are indicated by full circles. Combined SA–CRDS/FALP data at 100 K and 305 K (Refs. 8 and 34) are indicated by a full circle in a square. The temperature T in the SA–CRDS experiments is given by T_{Kin}, while in the FALP it is the temperature of the flow tube. That is why we use $T = 82$ K for data obtained in experiment made with discharge tube (SA–CRDS) immersed in liquid nitrogen, otherwise we indicate it as 77 K (e.g., in Fig. 5). Error bars (present CRDS data) represent statistical errors (see linear fits in Figs. 10 and 11). The dashed lines indicate the theoretical rate coefficients for para-H_3^+, ortho-H_3^+, and for H_3^+ ions in the thermal equilibrium (TDE).[6] The curves labeled CRR are the effective binary rate coefficients of collisional radiative recombination (CRR) calculated from the Stevefelt formula (see Refs. 31, 32, and 38) for electron densities $n_e = 5 \times 10^9$ cm^{-3} (dotted line) and $n_e = 3 \times 10^{10}$ cm^{-3} (dash-dotted line). For details see the Appendix.

Electron trap

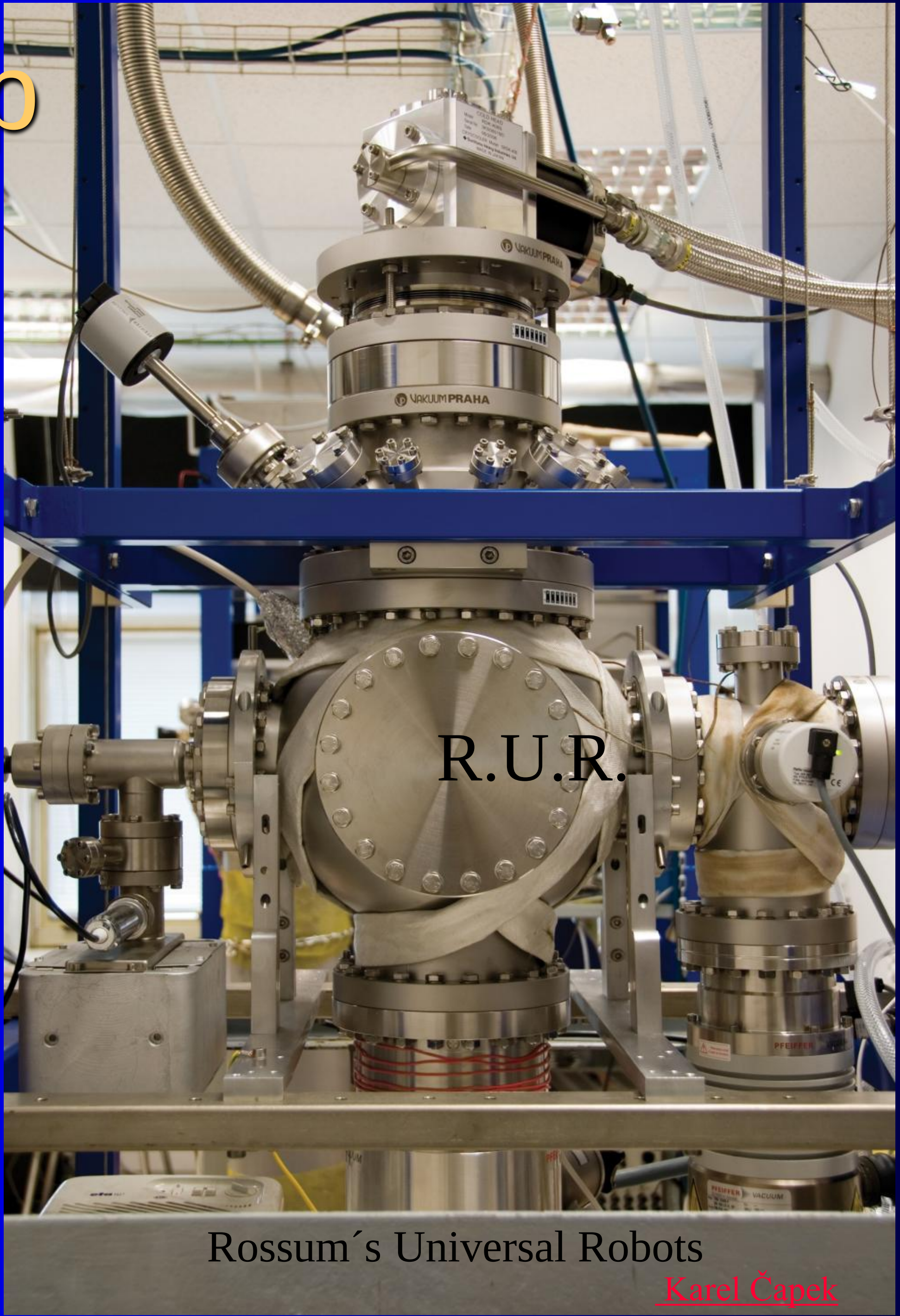

R.U.R.

Rossum´s Universal Robots

Karel Čapek